Dissecting the cellular basis of age-related cognitive dysfunction: Chronic chemogenetic inhibition of somatostatin-positive interneurons in the dentate gyrus hilus induces memory impairments

Jinrui Lyu[1], Rajasekar Nagarajan[1], Maltesh Kambali[1], Muxiao Wang[1], Uwe Rudolph[1,2,3]

[1]Department of Comparative Biosciences, College of Veterinary Medicine, University of Illinois at Urbana-Champaign, Urbana, IL 61801, USA

[2]Carl R. Woese Institute of Genomic Biology, University of Illinois at Urbana-Champaign, Urbana, IL 61801, USA

[3]Correspoding author: e-mail: urudolph@illinois.edu

Abstract

The cellular basis of age-related impairments of hippocampal function is not fully understood. In order to evaluate the role of somatostatin-positive (Sst^+) interneurons in the dentate gyrus hilus in this process, we chemogenetically inhibited Sst^+ interneurons in the dentate gyrus (DG) hilus. Chronic chemogenetic inhibition (CCI) of these neurons resulted in increased c-Fos staining in the DG hilus, a decrease in the percentage of Gad67- and of Sst-expressing neurons in the DG, and increased microglial activation in DG, CA3, and CA1. Total dendritic length and spine density were reduced in DG and CA1, suggesting reduced dendritic complexity. Behaviorally, the recognition index in an object recognition task and the percentage of spontaneous alternations in the Y maze were decreased, while in both initial and reversal learning in the Morris water maze the latencies to find the hidden platform were increased, suggesting cognitive dysfunction. Our findings establish a causal role for a reduced function of Sst^+ interneurons in the DG hilus for cognitive decline and suggest that this reduced function may contribute to age-related impairments of learning and memory. Our CCI mice may represent a cellularly defined model of hippocampal aging.

Introduction

Aging is an inevitable, complex, and multifactorial process. Cognitive decline, such as memory loss, is one of the most prevalent concerns in the aging population. Postoperative cognitive dysfunction (POCD) is a condition that may occur after surgery, especially in the elderly, resulting in increased morbidity and mortality (Steinmetz et al., 2009; Ancelin et al., 2010). It has also been argued that POCD might primarily be seen in people with preexisting age-related cognitive decline (Canet et al., 2003; Newman et al., 2007), so these phenomena might be interconnected. However, underlying causes are still poorly understood. Understanding the mechanism behind these phenomena might help devise therapeutic strategies against age-related cognitive decline and POCD.

The hippocampus plays a vital role in cognition, learning, and memory in the mammalian brain (Burgress 2002; Burgress et al., 2002; Shrager et al., 2007). Importantly, GABAergic interneurons in the hippocampus regulate memory processes (Spiegel et al., 2013). Optogenetic inhibition of hilar GABAergic interneuron activity impairs spatial memory (Andrews-Zwilling et al., 2012). Both aged humans and rodents displayed a lower performance with respect to hippocampal function, and a declined hippocampal interneuron activity (Stanley and Shetty 2004; Cadacio et al., 2003; Spalding et al., 2013; Oh et al., 2016). Moreover, many studies showed that aging in rodents is associated with DG and CA3 hyperactivity (Simkin et al., 2015), CA1 hypoactivity (Potier et al., 2006; Francavilla et al., 2020), and altered GABAergic signaling in the hippocampus (Bahadur Patel et al., 2021).

The dentate gyrus (DG), the first input-receiving region in the trisynaptic hippocampal pathway, is located between the entorhinal cortex and the CA3 region of the hippocampus (Hetherington et al., 1994). It receives information from the entorhinal cortex, projects to the CA3 pyramidal neurons, which then project to CA1 pyramidal neurons (Steward 1976; Deadwyler et al., 1975). DG granule cells encode spatial and contextual information (Ramirez et al., 2013). The tonic inhibition of DG granule cells, which are main regulators of hippocampal neuronal activity, controls pattern separation by distinguishing overlapping interferences into distinct and nonoverlapping information (Engin et al., 2015). α5 subunit-containing $GABA_A$ receptors ($\alpha5GABA_AR$), which are strongly expressed in the hippocampus, where they are primarily located extrasynaptically, mediate tonic inhibition in DG granule cells, CA1 and CA3 pyramidal cells (Engin et al., 2015; Glykys and Mody, 2006). Mice with a conditional knockout of $\alpha5GABA_AR$ in dentate gyrus granule cells, which display a reduced tonic inhibition but preserved phasic inhibition, perform worse in many behavioral tasks associated with high memory interference. These mice displayed increased c-Fos staining in DG and CA3, consistent with hyperactivity (Engin et al., 2015). Interestingly, as mentioned above, hyperactivity of DG and CA3 have also been reported in aging rodents (Oh et al., 2016), which implies that aging hippocampus may have similar or identical functional changes in activity levels.

Somatostatin (SST)-expressing neurons are a subpopulation of GABAergic interneurons (Viollet et al., 2008). It has been reported that Sst^+ interneurons regulate hippocampal networks through local inhibition, hyperpolarizing neurons, and reducing spine density (Yuan et al., 2017; Booker et al., 2018; Royer et al., 2012; Baratta et al., 2002; Hou and Yu 2013). Several studies demonstrate a correlation between neurodegenerative diseases and the loss of SST expression in the hippocampus. For example, patients with Alzheimer's disease (AD), which is associated with memory loss (Gahete et al., 2010), exhibit decreased SST expression in the brain (Tamminga et al., 1987), and GABAergic interneuron dysfunction (Andrews-Zwilling et al., 2010). Intravenous injection of SST into AD patients lead to an improvement of memory, and enhancement of visual processing and perception (Craft et al., 1999; Song et al., 2020; Vécsei et al., 1983). Moreover, after receiving

compounds that reduced hippocampal activity, both aged rats and human patients with amnestic mild cognitive impairment improved their memory (Bakker et al., 2012; Koh et al., 2010; Craft et al., 1999). Age-related cognitive deficits have been found to be correlated with a decrease in somatostatin-positive interneurons in the dentate gyrus hilus in rats (Spiegel et al., 2013). However, a causal relationship has not been demonstrated.

In this study, we examined whether suppression of the activity of hilar somatostatin-positive (Sst^+) interneurons is sufficient to induce defined learning and memory deficits, and whether this would occur with acute inhibition or require chronic inhibition. Our primary hypothesis was that only chronic inhibition of Sst^+ interneurons results in learning and memory deficits. We tested this hypothesis by generating and analyzing mice in which these neurons could be chemogenetically silenced by clozapine. If reduction of activity of Sst^+ interneurons in the dentate hilus resulted in cognitive dysfunction, the mice with such changes would potentially represent a novel mouse model of age-related cognitive decline, suggesting that normalizing impaired hippocampal inhibitory signaling might at least partially prevent or reverse POCD, which is primarily observed at higher ages.

Materials and Methods

Animals

Adult Sst-IRES-Cre transgenic mice (Stock no. 013044, The Jackson Laboratory) are crossed with C57BL/6J mice (Stock no. 000664, The Jackson Laboratory). Hemizygous adult mice of both sexes (3-4 months) were used for all studies. All mice were housed in a climate-controlled room maintained on a 12:12 light-dark cycle (lights on at 7 a.m., lights off at 7 p.m.) with food and water ad libitum. All procedures are approved by the Institutional Animal Care and Use Committee at University of Illinois at Urbana-Champaign.

Surgery

In order to study the role of Sst^+ in the dentate hilus, we generated mice in which the Sst^+ in the dentate hilus can be silenced chemogenetically.

Sst-Cre mice (3-4 months of age) received ketoprofen 5mg/kg, s.c. and atropine 0.04 mg/kg, s.c. before surgery. Mice were anesthetized with isoflurane (2-3%) and maintained under anesthesia (1.5%) throughout the surgery. AAV-hSyn-DIO-hM4D(Gi)-mCherry (Addgene #44362) was injected bilaterally into the DG hilus (stereotaxic coordinates AP: 2.1mm, ML: ±1.5mm, DV: -2.1mm relative to bregma) at a rate of 0.120 µL/min (1000nL per side), and the needle was left in place for an additional 2 mins to permit diffusion. The control groups were injected with an AAV vector, AAV-hSyn-DIO-mCherry (Addgene #50459), lacking the chemogenetic receptor hM4D(Gi). Injection locations were verified histologically at the end of the study.

Clozapine dihydrochloride (water soluble, Hello Bio #HB6129) was administered to the mice to activate hM4D(Gi) and thus inhibit hilar Sst^+ interneurons. The chronic treatment and control groups received clozapine (0.1mg/kg/day) in the drinking water for 21 days before and throughout all testing and the acute treatment and control groups groups were administered clozapine (0.1mg/kg i.p.) 30 min before behavioral experiments started. Mice drink approximately 4 mL of water per day. Males weigh more than females (e.g., 35 g versus 25 g, so the males may get 3,5 ug/4ml and the females 2.5 ug/4ml). Mice are weighed every 2 days, and the clozapine solution adjustments may be made every 2 days to reach the desired concentration.

Behavioral Tests
All behavioral experiments were performed during the light phase of the light/dark cycle. All mouse behaviors were monitored using the EthoVision XT videotracking system.

Novel Object Recognition Task
Mice were habituated in the experimental chamber for two days before the testing phase and each habituation period lasted for 15 min for each animal per session. Each mouse was presented with two identical objects for 10 min on the actual test day. After one hour, the mice were brought back to the same chamber and presented with one of the same training objects and one novel object. Interaction time was recorded using the multiple body point module to calculate the recognition index.

Morris Water Maze and Reversal Learning
A round pool (diameter: 120 cm) is filled with a mixture of water (22-24°C) and a white, non-toxic dye (Blick Premium Grade Tempera). A 10cm-diameter platform was submerged 2cm under the water surface. A 25cm-diameter target platform area was defined in the same quadrant as a concentric circle around the target platform. The frequency to enter and cumulative duration spent in the target platform are also recorded and analyzed. Visual cues were in the four quadrants of the pool in shapes with different geometry. Mice performed three trials daily from day 1 to day 7, released from a different quadrant each time in random order while the target platform location was constant. A trial ended when the animal found and stayed on the platform for 2 seconds. When an animal failed to reach the platform within 60 seconds, the experimenter guided it to the platform and put it back to the cage after staying on the platform for 10 seconds. From day 10 to day 13, the reversal learning phase was established by moving the platform from the original location to the nearest quadrant to increase the effects of interference. During probe trial (day 8) and reversal learning probe trial (day 14), the platform was removed, and the mice were left in the pool for 120 seconds.

Y-Maze Task
The apparatus was a Y-shaped maze with three gray, opaque plastic arms at a 120° angle from each other. The arm length is 31cm and the arm width is 7cm. Mice were placed in the center of the Y-Maze and allowed to explore any of the three closed arms freely for 8 min. The spontaneous arm alternation rate is calculated by dividing the number of spontaneous alternations by the number of total arm entries and multiplication by 100.

Perfusion
Mice were deeply anesthetized with ketamine (139 mg/kg i.p.) and xylazine (21 mg/kg i.p.) and then transcardially perfused with ice-cold phosphate-buffered saline (PBS) followed by 4% ice-cold paraformaldehyde. After 24 hours of post-fixation at 4°C, brains were moved into 30% sucrose for 72 hours and sectioned into 30 µm coronal sections using a cryostat. Free-floating sections were collected mounted on slides for staining.

Immunohistochemistry
We performed analysis of sections for target cell labeling and quantification. For analysis of c-Fos staining, all mice (n=6 per group) were exposed to a novel environment for 10 min and then placed into a clean cage individually for 1 hour before perfusion. For other stainings, free-floating sections (n=3 per sex, n=6 per group) were washed in 0.1 M phosphate-buffered saline (PBS) to remove cryoprotectant. The sections were blocked in blocking solution (2% NGS and 0.4% Triton X-100 in PBS) for 2 hours at room temperature, then incubated in the primary antibody at 4°C overnight. The primary antibodies used were as follows: rabbit anti-

c-Fos (Cell Signaling Tech, cat # 2250, 1:500), anti-somatostatin (SOM, Invitrogen, cat # PA5-82678, 1:1000), anti-glutamic acid decarboxylase 67 (GAD-67, Invitrogen, cat # PA5-213971:500), anti-IBA1 on microglia (IBA1, Invitrogen, cat # MA5-36257, 1:500), anti-neuronal nuclei (NeuN, Cell Signaling Tech, cat # 24307, 1:400).

After washing in blocking solution and 3% H_2O_2, the sections were incubated in a biotinylated goat anti-rabbit secondary antibody in blocking solution (Invitrogen, cat # 31820, 1:500) and transferred in a detection reagent (Vecstatin Elite ABC kit, Vector Laboratories, cat # PK-7200). The sections were incubated in a 3,3'-diaminobenzidine (DAB) solution. After rinsing, sections were mounted, dehydrated, and cover-slipped with mounting medium (Eukitt Quick-handling).

Golgi-Cox Staining

Mouse brains were removed from skulls without fixation. The fresh brain tissue was immersed in the impregnation solution (superGolgi Kit, Bioenno Tech) for 12 days and stored at 4°C in the dark. After being transferred to and incubated in the post-impregnation buffer for 2 days, the brain tissues were sectioned into 150µm thick sections using a vibratome. The sections were collected and mounted on gelatin-coated slides, dehydrated, and cleaned. Then they were cover-slipped using a mounting medium (Sigma-Aldrich) and stored at room temperature in the dark.

Dendritic Spine Analysis

We examined spines on apical dendrites of CA1 pyramidal neurons and dendrites of the dorsal dentate gyrus. To ensure the accurate measurements, we only evaluated dendrites that showed no breaks in the staining (Leuner et al., 2003) and that were not interrupted by other neurons or artifacts (Liu et al., 2001). Primary spines were not analyzed, we only evaluated spines located on secondary or tertiary dendritic trees. One segment per individual dendritic branch and two branches per neuron were chosen for the analysis. Quantitative two-dimensional analyses of dendritic and spine fragments were conducted by using a stereological microscope (Zeiss AxioImager A1 light microscope) with a 100x objective (oil immersion). For each dendrite at least 3 images along each spine segment were taken and spine densities calculated. Spine densities per 10µm and spine length from the dendrite shaft to the spine head were marked and calculated by using *Reconstruct* software (Version 1.1.0.1, Fiala, 2005).

Statistical Analysis

Statistical comparisons were performed using Graph Pad Prism (Graph Pad Software Inc., La Jolla, CA). In the c-Fos, SOM, GAD-67, and NeuN staining experiments, the average numbers of c-Fos$^+$ nuclei, Sst$^+$, GAD-67$^+$ cells, and NeuN$^+$ cells in the DG, CA3, and CA1 regions were analyzed using two-way repeated-measures analysis of variance (ANOVA). Each slide was counted three times, and the mean value was used in the ANOVAs. IBA1 staining was used as a marker for microglial activation. The average IBA1$^+$ density was analyzed with one-way ANOVA followed by Newman-Keuls multiple comparison tests. Statistical differences between treatments and regions were assessed using Bonferroni's post-hoc comparison test. Performance in behavioral experiments was be analyzed using one-way ANOVA and Scheffe's test.

Results

Chronic suppression of the activity of hilar Sst^+ interneurons leads to reduction of Sst^+ expression, GAD-67^+ expression, and increased microglial activation.

To validate of hilar Sst^+ interneuron manipulation, we performed immunofluorescence staining of coronal sections from experimental mice with DAPI counterstain and mCherry stain (**Fig. 1A**). All immunohistochemistry staining was done after behavioral studies (**Fig. 1B**).

In order to assess how a reduced activity of Sst^+ interneurons affects the activity of principal neurons in hippocampal subregions, we performed c-Fos staining in DG hilus, DG granule cell layer (GCL), CA3, and CA1 subregions of the hippocampus, for the purpose of analyzing the number of c-Fos-positive (c-Fos^+) cells.

We observed that in mice with a chronic chemogenetic inhibition of Sst^+ interneurons in the dentate gyrus (CCI) c-Fos staining in total DG and in DG hilus was increased ($p<0.001$, two-way ANOVA), consistent with hyperactivity, however, c-Fos staining in CA3 and CA1 was unaltered (**Fig. 2A**, top panel). In mice with an acute chemogenetic inhibition of Sst^+ in the dentate gyrus (ACI), c-Fos staining also increased in DG (hilus: $p < 0.05$; GCL: $p < 0.05$, two-way ANOVA), but not in CA3 and CA1 (**Fig. 2A**, bottom panel). This suggests that DG hilus-selective chronic inactivation of Sst^+ neurons leads to increased c-Fos^+ expression in the DG possibly due to reduced tonic inhibition due to lack of an inhibitory input. CCI manipulation resulted a 150% increase of c-Fos staining in the DG region (51% increase in the DG hilus) (**Fig. 2B**, left panel) while ACI manipulation resulted a 29% increase in the DG region (34% increase in the DG hilus, 24% increase in the DG GCL), which is an indication of hyperactivity in the DG region (**Fig. 2B**, right panel).

We then assessed the influence of chemogenetic inhibition of Sst^+ interneurons on the interneuronal markers Sst and GAD-67. While CCI mice displayed a significant decrease of Sst staining in DG hilus ($p<0.001$) and GCL ($p<0.01$) (**Fig. 3A,** top panel), GAD-67^+ was significantly decreased only in DG hilus ($p<0.01$, $t=3.675$, Diff= 9.540; DG GCL: $p> 0.05$, $t=2.568$, Diff= 2.568) (**Fig. 3B**, top panel). In ACI mice, no significant change was observed for both Sst^+ and GAD-67^+ staining ($p > 0.05$, two-way ANOVA) (**Fig. 3A, B**, bottom panels). We observed a loss of 51% of Sst^+ interneurons in the DG region (75% in the DG hilus, and 37% in the DG GCL) with the CCI treatment (**Fig. 3C**, left panel). For GAD-67^+ neurons, there is a 68% loss in the DG (64% loss in the DG hilus, and 74% loss in the DG GCL) (**Fig. 3C**, right panel).

Ionized Ca^{2+}-binding adapter protein 1 (IBA1) is an actin-interacting protein in microglia (Lituma et al., 2021; Badimon et al., 2020). We used IBA1 as a cellular marker for microglial activity to investigate whether chemogenetic inhibition led to hippocampal microglial activation by determining average cell body size in CCI and ACI mice (Spiegel et al., 2013). Whereas ACI did not result in changes in the microglial cell body size (**Fig. 4B**, right panel, $p> 0.05$), CCI resulted in an increased average microglial cell body size in DG ($q=5.821$, $p<0.001$), CA3 ($q=4.757$, $p<0.01$), and CA1 ($q=4.480$, $p<0.01$) (**Fig. 4B**, left panel). As a control experiment, we stained for $NeuN^+$, which is expressed by all neurons. Neither ACI nor CCI resulted in a change in the number of neurons (**Fig. 4A**. two-way ANOVA with Bonferroni post-test, $p> 0.05$). These data suggest a reduced expression of the markers Sst^+ and GAD-67^+ in DG hilar interneurons and in the DG granule cell layer in the absence of a loss of neurons, and that this change results in increased hippocampal microglial activation in DG, CA3 and CA1. As it has been reported recently that microglia is involved in negative feedback control of neuronal activity (Badimon et al., 2020), this microglial activation would be consistent with insufficient tonic inhibition via $GABA_A$Rs.

Reduced spine density and dendritic length in DG and CA1 after chronic and acute chemogenic inhibition of DG hilar Sst^+ interneurons

To evaluate the impact of chronic and acute chemogenic inhibition of DG hilar Sst^+ interneurons on hippocampal spine densities and spine length, we analyzed dendrites of granule cells located in the dentate gyrus and apical dendrites of CA1 pyramidal neurons (**Fig. 5A, B**). Four mouse brains were collected for Golgi-Cox staining from each treatment group. Quantification of dendritic length and spine density in DG and CA1 region was performed on 5-6 neurons per mouse using *Reconstruct* software.

Two-tailed *t*-test with Welch's correction of spine densities identified significant differences in DG between the AAV-mCherry group and the AAV-hM4D(Gi)-mCherry group (**Fig. 5C,** CCI: t=3.757, P=0.0027; **Fig. 5D**, ACI: t=2.704, P=0.0192), suggesting a decrease in spine density with chemogenetic inhibition of DG hilar Sst^+ interneurons. A significant decrease was observed in the AAV-hM4D(Gi)-mCherry group comparing to the AAV-hM4D(Gi) group in the apical CA1 region only after CCI (t=3.698, P=0.0027), but not after ACI (t=1.345, P=0.1962) **(Fig. 5C,D)**. However, total dendritic length was significantly reduced after ACI and CCI (**Fig. 5 E**, DG in CCI: t=3.435, P=0.009; CA1 in CCI: t=2.065, P=0.0410; **Fig. 5 F**, DG in ACI: t=3.328, P=0.0014; CA1 in ACI: t=2.166, P=0.0327), indicating a reduction in total dendritic length in DG and apical CA1 after chronic and acute inhibition of DG hilar Sst^+ interneurons.

Dendritic spines are often categorized by their various morphological subpopulations, such as stubby, mushroom, thin, and long thin (**Fig 5H**). We found a significant reduction of mushroom spines with other morphological types of spine unchanged (**Fig 5G**; two-way ANOVA, group × spine type, $F_{(3,40)}=2.25$, t=2.737, P<0.05). CCI resulted in a reduced number of mushroom spines, which are associated with long-term memory storage (Bourne and Harris, 2007).

Cognitive deficits in mice with chemogenetically reduced activity of somatostatin-positive interneurons in the dentate hilus.

Cognitive function has previously been reported to decline with aging in mice (Ingram et al., 1988). To examine the impact of reduced activity of Sst^+ interneurons, specifically potential reductions in cognitive functions, we performed the novel object recognition task (NOR), the Morris water maze test (MWM) including reversal learning, and the Y-Maze task (YM) in both ACI and CCI experiments **(Fig. 1B)**. It has been demonstrated before that performance in the NOR and the MWM is linked to CA1 (Engin et al., 2020; Tsien et al., 1996; Lee and Kesner 2002; Kesner et al., 2019), whereas reversal learning is linked to the dentate gyrus (Engin et al., 2015).

To investigate the potential spatial memory deficits in the experimental mice, we performed the MWM (CCI: n=11-15; ACI: n=15; **Fig. 6**). A two-way mixed ANOVA followed by Bonferroni post-test was conducted to investigate the impact of "genotype" (AAV-hM4D(Gi)-mCherry v.s. AAV-mCherry) and day on two behavioral measures, path length and latency to find the hidden platform during learning (L) and reversal learning phases (RL). In CCI (**Fig. 6A-F**), the AAV-hM4D(Gi)-mCherry mice showed significantly increased path length (L: day, day × genotype, $F_{(5,76)}=1.547$, $p < 0.01$; $t_{(7)}=2.773$, $p < 0.05$ for day 3. RL: day, day × genotype, $F_{(4,76)}=1.575$, $p < 0.01$; $t_{(5)}=4.540$, $p < 0.001$ for day 9; $t_{(5)}=2.837$, $p < 0.05$ for day 11, $t_{(5)}=3.547$, $p < 0.01$ for day 13) (**Fig. 6A**) and longer latency to find the hidden platform (L: day × genotype, $F_{(5,76)}=1.591$, $p < 0.01$; $t_{(7)}=2.813$, $p < 0.05$ for day 6; $t_{(7)}=4.70$, $p < 0.001$ for day 7. RL: day × genotype, $F_{(4,76)}=2.634$, $p < 0.0001$; $t_{(5)} > 2$, $p < 0.01$ for days 9,10,12,13) (**Fig. 6B**). In ACI, the AAV-hM4D(Gi)-mCherry mice did not differ from AAV-mCherry mice in their performance; no significant difference in latency nor path length to find the hidden platform were observed in AAV-mCherry and AAV-hM4D

(Gi)-mCherry mice (path length: $F_{(1,94)}$=0.8596, p > 0.05, **Fig. 6G**; latency to find the hidden platform: $F_{(1,94)}$=1.082, p > 0.05, **Fig. 6H**).

After the initial learning phase and after the reversal learning phase, we conducted probe trials to determine memory retrieval ability in experimental mice. In the CCI learning probe trial, the AAV-hM4D(Gi)-mCherry mice displayed no significant difference for cumulative duration spent in the target platform area (unpaired t-test, p > 0.05, **Fig. 6C**) or frequency to enter the target platform area (unpaired t-test, p > 0.05, **Fig. 6D**). In the CCI reversal learning probe trial, the AAV-hM4D(Gi)-mCherry mice spent a significantly shorter time than the AAV-mCherry mice in the target quadrant (**Fig. 6E**) (unpaired t-test, AAV-hM4D(Gi)- mCherry: 7.708 ± 0.9183 n=11; AAV-mCherry: 3.825 ± 0.8063 n=15; p =0.3680), but the frequency to enter the target quadrant was not different (unpaired t-test, p > 0.05, **Fig. 6F**).

In the ACI learning probe trial, the AAV-hM4D(Gi)-mCherry mice displayed no significant difference for cumulative duration in the target platform area and the frequency to enter the target platform area (unpaired t-test, p > 0.05, **Fig. 6I, J**). In the ACI reversal learning probe trial, the AAV-hM4D(Gi)-mCherry mice displayed no significant difference for cumulative duration and frequency to enter the target platform area (unpaired t-test, p > 0.05, **Fig. 6K,L**). The performance in the MWM learning and reversal learning phases revealed that the experimental mice had impaired performance only under CCI, while the ACI treated experimental mice showed a relatively intact memory performance with no significant differences found in either path length or latency to find the hidden platform during learning, reversal learning, and probe trials.

We then determined whether loss of Sst^+ interneurons in the DG hilus is associated with a decline in short-term recognition memory by analyzing AAV-hM4D (Gi)-mCherry and AAV-mCherry mice during both CCI and ACI in the NOR test. A two-day habituation enabled mice to habituate to the arena. Mice were considered exploring the novel object when the nose point as defined by the EthoVision XT software was in close proximity to the object. A novelty recognition index was calculated by dividing the time spent in the proximity of the novel object by the total time spent with both objects. A significant decrease in the recognition index was observed in CCI (AAV-hM4D (Gi)-mCherry: 62.65 ± 3.406, n=8; AAV-mCherry: 48.12 ± 4.352, n=6; p < 0.05, unpaired t-test, **Fig. 7A**). In contrast, both ACI AAV-hM4D (Gi)-mCherry mice and ACI AAV-mCherry mice spent a similar amount of time in the proximity of the novel object (hM4D (Gi)-mCherry: 51.77 ± 3.489, n=8; mCherry: 59.63 ± 2.752, n=8; p > 0.05, unpaired t-test; **Fig. 7B**), suggesting a decreased recognition memory in CCI AAV-hM4D (Gi)-mCherry mice.

The Y-maze task was used to assess short-term working memory. Mice with intact working memory would run in the three arms with spontaneous alternations, meaning that at each left-right decision point, they make an alternating decision. In the YM, a spontaneous alternation rate of 50% would imply random choices. In the CCI condition, AAV-hM4D(Gi)-mCherry mice had a significantly lower spontaneous alternation rate (AAV-mCherry: 58.91 ± 2.005 %, n=9; AAV-hM4D (Gi)-mCherry: 52.06 ± 1.811 %, n=6; p < 0.01, unpaired t-test) (**Fig. 7C**). In ACI, the spontaneous alternation rate also differed between groups with a lower recognition index in AAV-hM4D(Gi)-mCherry mice (AAV-mCherry: 63.31 ± 2.004, n=8; AAV-hM4D (Gi)-mCherry: 51.89 ± 1.362, n=9; P<0.0001; unpaired t-test) (**Fig. 7D**). Thus, the experimental (AAV-hM4D (Gi)-mCherry) mice had a significantly lower Y-maze spontaneous alternation rate than control (AAV-mCherry) mice in both ACI and CCI conditions.

Discussion

Understanding the cellular mechanism underlying aging is crucial to develop novel strategies to prevent or to reverse age-related cognitive dysfunction. Based on previous studies in aged rats, which showed that both Sst and GAD-67 proteins in DG hilus interneurons are reduced with age (Spiegel et al., 2013) and that the reduction of DG hilar Sst^+ is correlated with cognitive impairments (Spiegel et al., 2013; Koh et al., 2014), we investigated two main questions: whether a reduced activity of Sst^+ interneurons in the DG hilus would be sufficient to affect the activity of principal neurons in hippocampal subregions and whether acute and chronic suppression of the activity of hilar Sst^+ interneurons would impair defined learning and memory functions differently.

Silencing Sst^+ Cell Function in the DG Hilus

To achieve a Sst^+ cell-specific manipulation, we used somatostatin-IRES-Cre (Sst-Cre) mice, which express Cre recombinase in somatostatin-expressing neurons. We bred heterozygous Sst-Cre mice with wildtype mice to generate experimental Sst-Cre mice. A G_i-coupled designer receptor exclusively activated by designer drugs (DREADD) was used that decreases the overall amount of cAMP, which results in neural inhibition (Roth 2016; Gomez et al., 2017). To achieve region-selective manipulation, we stereotaxically injected the G_i-DREADD construct that will only be expressed in Cre-positive cells into the dentate gyrus hilus region, where it can be activated with clozapine N-oxide (CNO) or clozapine. While CNO is likely the most widely used ligand for chemogenetic studies, clozapine displays higher affinity and greater potency for hM4D(Gi) (Gomez et al., 2017). Clozapine has favorable pharmacokinetic properties for chronic administration (Jendryka et al., 2019, Cho et al., 2020) and was therefore used in our experiments.

While the current study was underway, Fee et al. (2021) reported a study on the role of Sst^+ cells in regulating mood and cognitive functions. Instead of investigating the role of Sst^+ cell in a targeted region, e.g., in our current study the DG hilus, they used a more generalized approach and developed a chemogenetic model which inhibits Sst^+ interneuron function brain-wide by injecting their chemogenetic viral construct intraventricularly. They employed CNO to activate the DREADD instead of clozapine and also performed the YM and NOR tasks. They achieved repeated acute silencing of Sst^+ cells by administrating CNO 30 minutes before each behavioral experiment, which is similar to our ACI model. While they found that their CNO-treated mice spent significantly less time with the novel object than with the familiar object in the NOR task and no differences between groups in the YM task, with acute injections of clozapine we found no difference between AAV-mCherry-injected mice and AAV-hM4D(Gi)-mCherry-injected mice in the NOR task, but AAV-hM4D(Gi)-mCherry-injected mice displayed significantly fewer spontaneous alternations in the YM task. Although the reasons for the observed differences are not understood, there are some potential explanations. Their cognitive deficits were induced by repeated acute CNO injections across nine behavioral tasks, including YM and NOR tasks. We used the same daily amount of clozapine (0.1mg/kg) in CCI and ACI, whereas Fee et al. (2021) used 3.5 mg/kg CNO per day. As stated above, compared to CNO, clozapine is more potent and has a longer half-life (Gomez et al., 2017; Jendryka et al., 2019). Moreover, their generalized Sst^+ interneuron inhibition could result in different adaptations in multiple neural circuits compared to our region-specific Sst^+ cell inhibition. Their brain-wide Sst^+ interneuron silencing might result in global and thus somewhat unspecific effects, which may result in different behavioral findings comparing to ours. Our current study has the limitation that we did not exclude the possibility that the chemogenetic receptor hM4D(Gi) might be active in the absence of clozapine, but even if these were the case, it would not invalidate our results as

we are clearly seeing significant differences with hM4D(Gi) compared to the viral control construct after administration of clozapine. In contrast, Fee et al. injected vehicle and CNO into their mice injected with an hM4D(Gi) construct. This, however, makes it difficult to distinguish between CNO effects on the DREADD and effects that CNO may have on its own (MacLaren et al., 2016). In contrast, our experiments, in which all groups are treated with clozapine control for effects that clozapine may have on its own. In any case, both studies demonstrated effects of Sst^+ cell regulation on short-term memory and cognitive functions.

Reduced activity of somatostatin-positive interneurons in the dentate gyrus hilus and cognitive deficits

Behavioral experimental results showed that chronic suppression of the activity of hilar Sst^+ interneurons leads to cognitive dysfunction. Chronic treatment with clozapine resulted in a decreased recognition index in the NOR. In addition, an increased path length and increased latency to find the hidden platform in the MWM have been observed with the chronic treatment, both for learning and reversal learning. In contrast, performance in these tasks was not altered by acute treatment with clozapine. In the YM, both acute and chronic treatments with clozapine showed significantly lower YM spontaneous alternation rates in the AAV-hM4D(Gi)-mCherry mice, indicating memory impairment. The AAV-hM4D(Gi)-mCherry mice visited the novel, undiscovered arm significantly less frequently with both acute and chronic chemogenetic manipulations and thus showed impaired spatial memory. The mice in the control group stereotaxically injected with AAV-hSyn-DIO-mCherry but treated with clozapine performed better at spontaneous arm alternations, i.e., choosing a different direction at each decision point.

While MWM learning and reversal learning and NOR are hippocampal-dependent tasks; multiple brain regions, including the hippocampus, prefrontal cortex, and basal forebrain are thought to be involved in YM performance. Andrews-Zwilling et al. (2012) inhibited hilar GABAergic interneuron optogenetically and found these mice performed worse in spatial learning and memory retrieval tasks but, surprisingly, displayed an unaltered behavior in the YM task. One major difference to the current study is that Andrews-Zwilling et al. were apparently targeting all GABAergic interneurons in the DG hilus, not just the Sst^+ interneurons that we have targeted in the current study. Our YM data indicate that both the acute and chronic chemogenetic inhibition result in cognitive deficits. Indeed, when considering chronic chemogenetic inhibition as a potential model for hippocampal aging, our results are in line with previous studies which showed memory impairments in both MWM and NOR in aged rodents (Dong et al., 2018; Hamieh et al., 2021; Shukla et al., 2019), indicating that memory impairment and aging are closely linked and may be dependent on the same hippocampal neural circuits (Tsien et al., 1996; Engin et al., 2015; Rampon et al., 2000).

Molecular and cellular analysis of chronic and acute inhibition of somatostatin-positive interneurons in the dentate gyrus hilus

Several lines of evidence point to a role of GABAergic inhibition for hippocampal learning and memory. In mice in which hilar GABAergic interneurons were silenced optogenetically, c-Fos^+ expression in the DG (but not in CA3 or CA1) and the firing rate of the GCs were increased, resulting in impaired spatial learning and memory retrieval (Andrews-Zwilling et al., 2012). Aged rats with memory impairment had restoration of hilar Sst expression after receiving levetiracetam, a compound that modulates synaptic neurotransmitter release (Spiegel et al., 2013). Mice with decreased GABA levels in the hippocampus induced by overexpressing GABA transporter 1, which is mediating GABA reuptake, display deficits in

learning and memory (Hu et al., 2004). A lack of α5GABA$_A$R in the DG GCL, which led to a reduced inhibitory input into the granule cells, has previously been shown to also result in a reduced tonic inhibition (Engin et al., 2015). These studies reveal the critical role of GABAergic neurotransmission for hippocampal learning.
The c-Fos gene is a cellular proto-oncogene that can be triggered by neuronal activation, cAMP pathway stimulation, and Ca^{2+} elevation in the brain (Hudson et al., 2018). Here, we used c-Fos as a marker for neuronal activity in the hippocampus and found increased c-Fos expression elicited by inhibition of Sst^+ DG hilar interneurons only in the DG, but neither in the DG GCL layer nor in CA3 or CA1 after CCI. This finding indicated that increased c-Fos-activity in the DG correlates with the cognitive impairment stated above. However, our experiments with ACI show that increased c-Fos activity in the DG h is not sufficient for the cognitive impairments seen in the NOR and the MWM.

GABA-mediated inhibition is important component of neuronal circuits involved in modulating memory functions. Age-related cognitive dysfunction is attributable to altered GABAergic signaling in the hippocampus and the prefrontal cortex (McQuail et al., 2015; Porges et al., 2017). The number of GABA-immunoreactive neurons declines with age in the DG and CA3 regions (Spiegel et al., 2013). Baseline GABA, GABA release, and GABA receptor binding are also reduced with aging (Caspary et al., 1995). Taurine, an agonist of GABA$_A$R, improved learning and retention in aged mice, potentially by promoting the GABAergic activity of Sst^+ interneurons (El Idrissi 2008). We found a significantly lower Sst^+ expression in the DG only with our CCI (and not with our ACI) manipulation, indicating that some Sst^+ interneurons loose somatostatin expression, and this loss correlates with the observed memory deficits and not with c-Fos staining in the DG, which was also increased in the ACI model. GAD-67 is an enzyme responsible for GABA synthesis and a decreased number of GAD-67$^+$ interneurons in the DG hilus is associated with memory impairments (Spiegel et al., 2013).

Aging is associated with the loss of GAD-67-positive interneurons in the DG and CA3 region (Stanley and Shetty 2004). We found significantly reduced GAD-67 expression in DG hilus in CCI AAV-hM4D(Gi)-mCherry mice, suggesting that in this respect our CCI model replicates observations in aging animals. Interestingly, a difference between acute and chronic chemogenetic silencing of Sst^+ interneurons has also been reported by Soumier and Sibille (2014), who described that while acute chemogenetic inhibition of Sst^+ interneurons in the frontal cortex resulted in increased emotional behavioral emotionality, chronic chemogenetic inhibition resulted in decreased behavioral emotionality.

Increased microglia activation was shown to be associated with human aging (Tay et al., 2017). In our study, we found microglial activation in DG, CA3, and CA1 regions in CCI mice, indicating the inactivation of Sst^+ interneurons cause changes in the hippocampus that even result in an increase of neuroinflammation markers. With the unchanged number of total hilar and hippocampal $NeuN^+$ neurons, the decline in other markers, specifically Sst and GAD-67 most likely indicates a loss of target protein but not neuronal cell death (Spiegel et al., 2013).

The results of our study provide novel evidence that chronic (but not acute) inhibition of hilar Sst^+ interneurons lead to in a reduction of Sst expression in the DG hilus and increased microglial activation. Mice with chronic suppression of hilar Sst^+ interneurons may be a model of age-related cognitive deficits. Unlike the acute chemogenetic inhibition model which results in increased c-Fos staining and hyperactivity in DG, the chronic chemogenetic inhibition model mimics some relevant features of hippocampal aging and may thus be further evaluated as an experimental model of aging-related processes in the hippocampus. This novel model may also be useful to study POCD and other age-related cognitive disorders, and hopefully to develop a novel therapeutic approach to prevent or reverse POCD

in the elderly. Taken together, our experiments demonstrate a causal relationship between a chronic loss of activity of dentate hilus Sst^+ interneurons, microglial activation, and cognitive dysfunction.

Chemogenetic inhibition of DG hilar somatostatin-positive interneurons reduced spine densities and dendritic length in DG and CA1

Dendritic spines are the primary sites of most excitatory synapses on pyramidal neurons. In neuropsychiatric conditions that affect cognitive function, the morphology and density of dendritic spines are altered (Penzes et al., 2011). Alterations in neuronal morphology occur in the hippocampus during normal aging and are related to memory and cognitive impairment (Rosenzewig and Barnes, 2003). Loss of dendritic spines was observed in AD post-mortem human brains and Amyloid Precursor Protein overexpressing mice (Moolman et al., 2004). Spatial training increases spine densities of CA1 and DG neurons, which goes along with better learning abilities (Moser et al., 1994; von Bohlen und Halbach et al., 2006), indicating that some forms of learning and memory result in an increased number of dendritic spines. In the present study, a reduction of spine density and total dendritic length, induced by acute and chronic chemogenetic inhibition of somatostatin-positive interneurons in the DG hilus may underlie cognitive declines seen in behavioral tasks reported in this study. This is reminiscent of the finding that in age-related neuronal atrophy, as evidenced by dendritic shrinkage and spine loss in frontal cortex and hippocampus, a memory deficit in Y-maze alternation task has been described (Prevot et al., 2020). This observation is also in line with our chronic chemogenetic inhibition model being a potential model of hippocampal aging.

Spine density increases with formation of long-term memory, implicating a role of spine dynamics in cognition (Kasai et al., 2010). The reduction in spine densities and dendritic length in apical CA1 and DG were observed after both ACI and CCI, suggesting that activation of the inhibitory hM4D(Gi) DREADD in the DG hilus even by acute injections of clozapine is sufficient to cause a reduction of spine density in DG. It is also possible that the repeated nature of our clozapine injections in the ACI group has indeed resulted in some chronic effects on dendritic spines. It is noteworthy, however, that the acute and chronic clozapine administration protocols had clearly different effects, e.g., in the MWM and the NOR tests and on microglial activation and on the number of Sst^+ and $Gad67^+$ interneurons, suggesting that these protocols were clearly distinct. The decreased number of mushroom spines, which have been termed “memory spines” (Bourne and Harris, 2007; Mahmmoud et al., 2015) in the DG after chronic chemogenetic inhibition of hilar Sst^+ interneurons supports the view that in changes in dendritic spine underly at least some of the cognitive deficits that we have observed.

Overall, our study revealed that in contrast to ACI, CCI of hilar Sst^+ interneurons leads to cognitive deficits in the NOR and the learning phase of the MWM, which are at least in part CA1-dependent tasks, and in the reversal learning phase of the MWM, which is a DG-dependent task, while ACI and CCI have similar effects in the YM. Thus, cognitive dysfunction in relatively hippocampus-specific tasks appears to be correlated with the observed reduction in the number of Sst^+ and GAD-67^+ interneurons. In addition, performance in the MWM and the NOR were correlated with a reduced dendritic spine density in CA1, while in DG dendritic spines are reduced by both CCI and ACI, which is reflective of the c-Fos-staining results and the performance in the YM. (**Table. 1, 2**).

Conclusion and Future Directions

In summary, we have shown a causal relationship between the inhibition of hilar Sst^+ interneurons and cognitive dysfunction which is similar to age-related cognitive dysfunction. Taking into account the known correlation between spatial memory and number of hilar

interneurons (Spiegel et al., 2013), chronic chemogenetic inhibition of hilar Sst^+ interneurons may be useful as a novel model of hippocampal aging, which may help in the study of POCD, which occurs mainly in aged individuals. This model also allows to study to which degree this specific and well-defined pathology contributes to age-related cognitive dysfunction.

Acknowledgements
Research reported in this manuscript was supported by the National Institute of General Medical Sciences of the National Institutes of Health under award number R01GM128183 and by institutional funds. The content is solely the responsibility of the authors and does not necessarily represent the official views of the National Institutes of Health.

Competing interests
UR serves on the Scientific Advisory Board of Damona Pharmaceuticals.

Author contributions
Conceptualization: UR
Investigation: JL
Analysis and Interpretation: JL, RN, UR
Methodology: JL, RN, MK, MW, UR
Funding acquisition: UR
Supervision: UR
Writing – original draft: JL, UR
Writing – review & editing: JL, RN, MK, MW, UR

References

1. Ancelin, M. L., de Roquefeuil, G., Scali, J., Bonnel, F., Adam, J. F., Cheminal, J. C., Cristol, J. P., Dupuy, A. M., Carrière, I., & Ritchie, K. (2010). Long-term post-operative cognitive decline in the elderly: the effects of anesthesia type, apolipoprotein E genotype, and clinical antecedents. *Journal of Alzheimer's disease : JAD*, *22 Suppl 3*, 105–113. https://doi.org/10.3233/JAD-2010-100807
2. Andrews-Zwilling, Y., Bien-Ly, N., Xu, Q., Li, G., Bernardo, A., Yoon, S. Y., Zwilling, D., Yan, T. X., Chen, L., & Huang, Y. (2010). Apolipoprotein E4 causes age- and Tau-dependent impairment of GABAergic interneurons, leading to learning and memory deficits in mice. *The Journal of neuroscience : the official journal of the Society for Neuroscience*, *30*(41), 13707–13717. https://doi.org/10.1523/JNEUROSCI.4040-10.2010
3. Andrews-Zwilling, Y., Gillespie, A. K., Kravitz, A. V., Nelson, A. B., Devidze, N., Lo, I., Yoon, S. Y., Bien-Ly, N., Ring, K., Zwilling, D., Potter, G. B., Rubenstein, J. L., Kreitzer, A. C., & Huang, Y. (2012). Hilar GABAergic interneuron activity controls spatial learning and memory retrieval. *PloS one*, *7*(7), e40555. https://doi.org/10.1371/journal.pone.0040555
4. Leuner, B., Falduto, J., & Shors, T. J. (2003). Associative memory formation increases the observation of dendritic spines in the hippocampus. *The Journal of neuroscience: the official journal of the Society for Neuroscience*, *23*(2), 659–665. https://doi.org/10.1523/JNEUROSCI.23-02-00659.2003
5. Badimon, A., Strasburger, H. J., Ayata, P., Chen, X., Nair, A., Ikegami, A., Hwang, P., Chan, A. T., Graves, S. M., Uweru, J. O., Ledderose, C., Kutlu, M. G., Wheeler, M. A., Kahan, A., Ishikawa, M., Wang, Y. C., Loh, Y. E., Jiang, J. X., Surmeier, D. J., Robson, S. C., … Schaefer, A. (2020). Negative feedback control of neuronal activity by microglia. *Nature*, *586*(7829), 417–423. https://doi.org/10.1038/s41586-020-2777-8
6. Bahadur Patel, A., Veeraiah, P., Shameem, M., Mahesh Kumar, J., & Saba, K. (2021). Impaired GABAergic and glutamatergic neurometabolic activity in aged mice brain as measured by ^{1}H-[^{13}C]-NMR spectroscopy. *FASEB journal: official publication of the Federation of American Societies for Experimental Biology*, *35*(2), e21321. https://doi.org/10.1096/fj.202001704RR
7. Bakker, A., Krauss, G. L., Albert, M. S., Speck, C. L., Jones, L. R., Stark, C. E., Yassa, M. A., Bassett, S. S., Shelton, A. L., & Gallagher, M. (2012). Reduction of hippocampal hyperactivity improves cognition in amnestic mild cognitive impairment. *Neuron*, *74*(3), 467–474. https://doi.org/10.1016/j.neuron.2012.03.023
8. Baratta, M. V., Lamp, T., & Tallent, M. K. (2002). Somatostatin depresses long-term potentiation and Ca2+ signaling in mouse dentate gyrus. *Journal of neurophysiology*, *88*(6), 3078–3086. https://doi.org/10.1152/jn.00398.2002
9. Booker, S. A., Loreth, D., Gee, A. L., Watanabe, M., Kind, P. C., Wyllie, D., Kulik, Á., & Vida, I. (2018). Postsynaptic $GABA_BRs$ Inhibit L-Type Calcium Channels and Abolish Long-Term Potentiation in Hippocampal Somatostatin Interneurons. *Cell reports*, *22*(1), 36–43. https://doi.org/10.1016/j.celrep.2017.12.021
10. Bourne J, Harris KM. Do thin spines learn to be mushroom spines that remember? Curr Opin Neurobiol. 2007 Jun;17(3):381-6. doi: 10.1016/j.conb.2007.04.009. Epub 2007 May 10. PMID: 17498943.
11. Burgess N. (2002). The hippocampus, space, and viewpoints in episodic memory. *The Quarterly journal of experimental psychology. A, Human experimental psychology*, *55*(4), 1057–1080. https://doi.org/10.1080/02724980244000224

12. Burgess, N., Maguire, E. A., & O'Keefe, J. (2002). The human hippocampus and spatial and episodic memory. *Neuron*, *35*(4), 625–641. https://doi.org/10.1016/s0896-6273(02)00830-9
13. Cadacio, C. L., Milner, T. A., Gallagher, M., & Pierce, J. P. (2003). Hilar neuropeptide Y interneuron loss in the aged rat hippocampal formation. *Experimental neurology*, *183*(1), 147–158. https://doi.org/10.1016/s0014-4886(03)00126-2
14. Canet, J., Raeder, J., Rasmussen, L. S., Enlund, M., Kuipers, H. M., Hanning, C. D., Jolles, J., Korttila, K., Siersma, V. D., Dodds, C., Abildstrom, H., Sneyd, J. R., Vila, P., Johnson, T., Muñoz Corsini, L., Silverstein, J. H., Nielsen, I. K., Moller, J. T., & ISPOCD2 investigators (2003). Cognitive dysfunction after minor surgery in the elderly. *Acta anaesthesiologica Scandinavica*, *47*(10), 1204–1210. https://doi.org/10.1046/j.1399-6576.2003.00238.
15. Cartin, L., Lounsbury, K. M., & Nelson, M. T. (2000). Coupling of Ca(2+) to CREB activation and gene expression in intact cerebral arteries from mouse : roles of ryanodine receptors and voltage-dependent Ca(2+) channels. *Circulation research*, *86*(7), 760–767. https://doi.org/10.1161/01.res.86.7.760
16. Caspary, D. M., Milbrandt, J. C., & Helfert, R. H. (1995). Central auditory aging: GABA changes in the inferior colliculus. *Experimental gerontology*, *30*(3-4), 349–360. https://doi.org/10.1016/0531-5565(94)00052-5
17. Cho, J., Ryu, S., Lee, S., Kim, J., & Kim, H. I. (2020). Optimizing clozapine for chemogenetic neuromodulation of somatosensory cortex. *Scientific reports*, *10*(1), 6001. https://doi.org/10.1038/s41598-020-62923-x
18. Craft, S., Asthana, S., Newcomer, J. W., Wilkinson, C. W., Matos, I. T., Baker, L. D., Cherrier, M., Lofgreen, C., Latendresse, S., Petrova, A., Plymate, S., Raskind, M., Grimwood, K., & Veith, R. C. (1999). Enhancement of memory in Alzheimer disease with insulin and somatostatin, but not glucose. *Archives of general psychiatry*, *56*(12), 1135–1140. https://doi.org/10.1001/archpsyc.56.12.1135
19. Deadwyler, S. A., West, J. R., Cotman, C. W., & Lynch, G. S. (1975). A neurophysiological analysis of commissural projections to dentate gyrus of the rat. *Journal of neurophysiology*, *38*(1), 167–184. https://doi.org/10.1152/jn.1975.38.1.167
20. Dong, Y., Guo, C. R., Chen, D., Chen, S. M., Peng, Y., Song, H., & Shi, J. R. (2018). Association between age-related hearing loss and cognitive decline in C57BL/6J mice. *Molecular medicine reports*, *18*(2), 1726–1732. https://doi.org/10.3892/mmr.2018.9118
21. El Idrissi A. (2008). Taurine improves learning and retention in aged mice. *Neuroscience letters*, *436*(1), 19–22. https://doi.org/10.1016/j.neulet.2008.02.070
22. Engin, E., Sigal, M., Benke, D., Zeller, A., & Rudolph, U. (2020). Bidirectional regulation of distinct memory domains by α5-subunit-containing $GABA_A$ receptors in CA1 pyramidal neurons. *Learning & memory (Cold Spring Harbor, N.Y.)*, *27*(10), 423–428. https://doi.org/10.1101/lm.052084.120
23. Engin, E., Zarnowska, E. D., Benke, D., Tsvetkov, E., Sigal, M., Keist, R., Bolshakov, V. Y., Pearce, R. A., & Rudolph, U. (2015). Tonic Inhibitory Control of Dentate Gyrus Granule Cells by α5-Containing GABAA Receptors Reduces Memory Interference. *The Journal of neuroscience : the official journal of the Society for Neuroscience*, *35*(40), 13698–13712. https://doi.org/10.1523/JNEUROSCI.1370-15.2015
24. Fiala J. C. (2005). Reconstruct: a free editor for serial section microscopy. *Journal of microscopy*, *218*(Pt 1), 52–61. https://doi.org/10.1111/j.1365-2818.2005.01466.x

25. Fee, C., Prevot, T. D., Misquitta, K., Knutson, D. E., Li, G., Mondal, P., Cook, J. M., Banasr, M., & Sibille, E. (2021). Behavioral Deficits Induced by Somatostatin-Positive GABA Neuron Silencing Are Rescued by Alpha 5 GABA-A Receptor Potentiation. *The international journal of neuropsychopharmacology*, *24*(6), 505–518. https://doi.org/10.1093/ijnp/pyab002
26. Francavilla, R., Guet-McCreight, A., Amalyan, S., Hui, C. W., Topolnik, D., Michaud, F., Marino, B., Tremblay, M. È., Skinner, F. K., & Topolnik, L. (2020). Alterations in Intrinsic and Synaptic Properties of Hippocampal CA1 VIP Interneurons During Aging. *Frontiers in cellular neuroscience*, *14*, 554405. https://doi.org/10.3389/fncel.2020.554405
27. Gahete, M. D., Rubio, A., Durán-Prado, M., Avila, J., Luque, R. M., & Castaño, J. P. (2010). Expression of Somatostatin, cortistatin, and their receptors, as well as dopamine receptors, but not of neprilysin, are reduced in the temporal lobe of Alzheimer's disease patients. *Journal of Alzheimer's disease : JAD*, *20*(2), 465–475. https://doi.org/10.3233/JAD-2010-1385
28. Glykys, J., & Mody, I. (2006). Hippocampal network hyperactivity after selective reduction of tonic inhibition in GABA A receptor alpha5 subunit-deficient mice. *Journal of neurophysiology*, *95*(5), 2796–2807. https://doi.org/10.1152/jn.01122.2005
29. Gomez, J. L., Bonaventura, J., Lesniak, W., Mathews, W. B., Sysa-Shah, P., Rodriguez, L. A., Ellis, R. J., Richie, C. T., Harvey, B. K., Dannals, R. F., Pomper, M. G., Bonci, A., & Michaelides, M. (2017). Chemogenetics revealed: DREADD occupancy and activation via converted clozapine. *Science (New York, N.Y.)*, *357*(6350), 503–507. https://doi.org/10.1126/science.aan2475
30. Hamieh, A. M., Camperos, E., Hernier, A. M., & Castagné, V. (2021). C57BL/6 mice as a preclinical model to study age-related cognitive deficits: Executive functions impairment and inter-individual differences. *Brain research*, *1751*, 147173. https://doi.org/10.1016/j.brainres.2020.147173
31. Hetherington, P. A., Austin, K. B., & Shapiro, M. L. (1994). Ipsilateral associational pathway in the dentate gyrus: an excitatory feedback system that supports N-methyl-D-aspartate-dependent long-term potentiation. *Hippocampus*, *4*(4), 422–438. https://doi.org/10.1002/hipo.450040405
32. Hou, Z. H., & Yu, X. (2013). Activity-regulated somatostatin expression reduces dendritic spine density and lowers excitatory synaptic transmission via postsynaptic somatostatin receptor 4. *The Journal of biological chemistry*, *288*(4), 2501–2509. https://doi.org/10.1074/jbc.M112.419051
33. Hu, J. H., Ma, Y. H., Jiang, J., Yang, N., Duan, S. H., Jiang, Z. H., Mei, Z. T., Fei, J., & Guo, L. H. (2004). Cognitive impairment in mice over-expressing gamma-aminobutyric acid transporter 1 (GAT1). *Neuroreport*, *15*(1), 9–12. https://doi.org/10.1097/00001756-200401190-00003
34. Hudson A. E. (2018). Genetic Reporters of Neuronal Activity: c-Fos and G-CaMP6. *Methods in enzymology*, *603*, 197–220. https://doi.org/10.1016/bs.mie.2018.01.023
35. Ingram D. K. (1988). Complex maze learning in rodents as a model of age-related memory impairment. *Neurobiology of aging*, *9*(5-6), 475–485. https://doi.org/10.1016/s0197-4580(88)80101-5
36. Jendryka, M., Palchaudhuri, M., Ursu, D., van der Veen, B., Liss, B., Kätzel, D., Nissen, W., & Pekcec, A. (2019). Pharmacokinetic and pharmacodynamic actions of clozapine-N-oxide, clozapine, and compound 21 in DREADD-based chemogenetics in mice. *Scientific reports*, *9*(1), 4522. https://doi.org/10.1038/s41598-019-41088-2

37. Kasai, H., Fukuda, M., Watanabe, S., Hayashi-Takagi, A., & Noguchi, J. (2010). Structural dynamics of dendritic spines in memory and cognition. *Trends in neurosciences*, *33*(3), 121–129. https://doi.org/10.1016/j.tins.2010.01.001
38. Kersten, M., Rabbe, T., Blome, R., Porath, K., Sellmann, T., Bien, C. G., Köhling, R., & Kirschstein, T. (2019). Novel Object Recognition in Rats With NMDAR Dysfunction in CA1 After Stereotactic Injection of Anti-NMDAR Encephalitis Cerebrospinal Fluid. *Frontiers in neurology*, *10*, 586. https://doi.org/10.3389/fneur.2019.00586
39. Koh, M. T., Haberman, R. P., Foti, S., McCown, T. J., & Gallagher, M. (2010). Treatment strategies targeting excess hippocampal activity benefit aged rats with cognitive impairment. *Neuropsychopharmacology : official publication of the American College of Neuropsychopharmacology*, *35*(4), 1016–1025. https://doi.org/10.1038/npp.2009.207
40. Koh, M. T., Spiegel, A. M., & Gallagher, M. (2014). Age-associated changes in hippocampal-dependent cognition in Diversity Outbred mice. *Hippocampus*, *24*(11), 1300–1307. https://doi.org/10.1002/hipo.22311
41. Lee, I., & Kesner, R. P. (2002). Differential contribution of NMDA receptors in hippocampal subregions to spatial working memory. *Nature neuroscience*, *5*(2), 162–168. https://doi.org/10.1038/nn790
42. Leuner, B., Falduto, J., & Shors, T. J. (2003). Associative memory formation increases the observation of dendritic spines in the hippocampus. *The Journal of neuroscience : the official journal of the Society for Neuroscience*, *23*(2), 659–665. https://doi.org/10.1523/JNEUROSCI.23-02-00659.2003
43. Lituma, P. J., Woo, E., O'Hara, B. F., Castillo, P. E., Sibinga, N., & Nandi, S. (2021). Altered synaptic connectivity and brain function in mice lacking microglial adapter protein Iba1. *Proceedings of the National Academy of Sciences of the United States of America*, *118*(46), e2115539118. https://doi.org/10.1073/pnas.2115539118
44. Liu, W. S., Pesold, C., Rodriguez, M. A., Carboni, G., Auta, J., Lacor, P., Larson, J., Condie, B. G., Guidotti, A., & Costa, E. (2001). Down-regulation of dendritic spine and glutamic acid decarboxylase 67 expressions in the reelin haploinsufficient heterozygous reeler mouse. *Proceedings of the National Academy of Sciences of the United States of America*, *98*(6), 3477–3482. https://doi.org/10.1073/pnas.051614698
45. MacLaren, D. A., Browne, R. W., Shaw, J. K., Krishnan Radhakrishnan, S., Khare, P., España, R. A., & Clark, S. D. (2016). Clozapine N-Oxide Administration Produces Behavioral Effects in Long-Evans Rats: Implications for Designing DREADD Experiments. *eNeuro*, *3*(5), ENEURO.0219-16.2016.
46. Mahmmoud, R. R., Sase, S., Aher, Y. D., Sase, A., Gröger, M., Mokhtar, M., Höger, H., & Lubec, G. (2015). Spatial and Working Memory Is Linked to Spine Density and Mushroom Spines. *PloS one*, *10*(10), e0139739. https://doi.org/10.1371/journal.pone.0139739
47. McQuail, J. A., Frazier, C. J., & Bizon, J. L. (2015). Molecular aspects of age-related cognitive decline: the role of GABA signaling. *Trends in molecular medicine*, *21*(7), 450–460. https://doi.org/10.1016/j.molmed.2015.05.002
48. Moolman DL, Vitolo OV, Vonsattel JP, Shelanski ML. Dendrite and dendritic spine alterations in Alzheimer models. J Neurocytol. 2004 May;33(3):377-87. doi: 10.1023/B:NEUR.0000044197.83514.64. PMID: 15475691.
49. Moser, M. B., Trommald, M., & Andersen, P. (1994). An increase in dendritic spine density on hippocampal CA1 pyramidal cells following spatial learning in adult rats suggests the formation of new synapses. *Proceedings of the National Academy of*

Sciences of the United States of America, *91*(26), 12673–12675. https://doi.org/10.1073/pnas.91.26.12673
50. Newman, S., Stygall, J., Hirani, S., Shaefi, S., & Maze, M. (2007). Postoperative cognitive dysfunction after noncardiac surgery: a systematic review. *Anesthesiology*, *106*(3), 572–590. https://doi.org/10.1097/00000542-200703000-00023
51. Oh, M. M., Simkin, D., & Disterhoft, J. F. (2016). Intrinsic Hippocampal Excitability Changes of Opposite Signs and Different Origins in CA1 and CA3 Pyramidal Neurons Underlie Aging-Related Cognitive Deficits. *Frontiers in systems neuroscience*, *10*, 52. https://doi.org/10.3389/fnsys.2016.00052
52. Penzes, P., Cahill, M. E., Jones, K. A., VanLeeuwen, J. E., & Woolfrey, K. M. (2011). Dendritic spine pathology in neuropsychiatric disorders. *Nature neuroscience*, *14*(3), 285–293. https://doi.org/10.1038/nn.2741
53. Pietronigro, E., Zenaro, E., Bianca, V. D., Dusi, S., Terrabuio, E., Iannoto, G., Slanzi, A., Ghasemi, S., Nagarajan, R., Piacentino, G., Tosadori, G., Rossi, B., & Constantin, G. (2019). Blockade of α4 integrins reduces leukocyte-endothelial interactions in cerebral vessels and improves memory in a mouse model of Alzheimer's disease. *Scientific reports*, *9*(1), 12055. https://doi.org/10.1038/s41598-019-48538-x
54. Porges, E. C., Woods, A. J., Edden, R. A., Puts, N. A., Harris, A. D., Chen, H., Garcia, A. M., Seider, T. R., Lamb, D. G., Williamson, J. B., & Cohen, R. A. (2017). Frontal Gamma-Aminobutyric Acid Concentrations Are Associated With Cognitive Performance in Older Adults. *Biological psychiatry. Cognitive neuroscience and neuroimaging*, *2*(1), 38–44. https://doi.org/10.1016/j.bpsc.2016.06.004
55. Potier, B., Jouvenceau, A., Epelbaum, J., & Dutar, P. (2006). Age-related alterations of GABAergic input to CA1 pyramidal neurons and its control by nicotinic acetylcholine receptors in rat hippocampus. *Neuroscience*, *142*(1), 187–201. https://doi.org/10.1016/j.neuroscience.2006.06.040
56. Prevot, T. D., Sumitomo, A., Tomoda, T., Knutson, D. E., Li, G., Mondal, P., Banasr, M., Cook, J. M., & Sibille, E. (2021). Reversal of Age-Related Neuronal Atrophy by α5-GABAA Receptor Positive Allosteric Modulation. *Cerebral cortex (New York, N.Y. : 1991)*, *31*(2), 1395–1408. https://doi.org/10.1093/cercor/bhaa310
57. Ramirez, S., Liu, X., Lin, P. A., Suh, J., Pignatelli, M., Redondo, R. L., Ryan, T. J., & Tonegawa, S. (2013). Creating a false memory in the hippocampus. *Science (New York, N.Y.)*, *341*(6144), 387–391. https://doi.org/10.1126/science.1239073
58. Rampon, C., Tang, Y. P., Goodhouse, J., Shimizu, E., Kyin, M., & Tsien, J. Z. (2000). Enrichment induces structural changes and recovery from nonspatial memory deficits in CA1 NMDAR1-knockout mice. *Nature neuroscience*, *3*(3), 238–244. https://doi.org/10.1038/72945
59. Rosenzweig ES, Barnes CA. Impact of aging on hippocampal function: plasticity, network dynamics, and cognition. Prog Neurobiol. 2003 Feb;69(3):143-79. doi: 10.1016/s0301-0082(02)00126-0. PMID: 12758108.
60. Roth B. L. (2016). DREADDs for Neuroscientists. *Neuron*, *89*(4), 683–694. https://doi.org/10.1016/j.neuron.2016.01.040
61. Royer, S., Zemelman, B. V., Losonczy, A., Kim, J., Chance, F., Magee, J. C., & Buzsáki, G. (2012). Control of timing, rate and bursts of hippocampal place cells by dendritic and somatic inhibition. *Nature neuroscience*, *15*(5), 769–775. https://doi.org/10.1038/nn.3077
62. Shrager, Y., Bayley, P. J., Bontempi, B., Hopkins, R. O., & Squire, L. R. (2007). Spatial memory and the human hippocampus. Proc. Natl. Acad. Sci. U.S.A., 104(8), 2961– 2966.

63. Shukla, R., Prevot, T. D., French, L., Isserlin, R., Rocco, B. R., Banasr, M., Bader, G. D., & Sibille, E. (2019). The Relative Contributions of Cell-Dependent Cortical Microcircuit Aging to Cognition and Anxiety. *Biological psychiatry*, *85*(3), 257–267. https://doi.org/10.1016/j.biopsych.2018.09.019
64. Simkin, D., Hattori, S., Ybarra, N., Musial, T. F., Buss, E. W., Richter, H., Oh, M. M., Nicholson, D. A., & Disterhoft, J. F. (2015). Aging-Related Hyperexcitability in CA3 Pyramidal Neurons Is Mediated by Enhanced A-Type K+ Channel Function and Expression. *The Journal of neuroscience: the official journal of the Society for Neuroscience*, *35*(38), 13206–13218. https://doi.org/10.1523/JNEUROSCI.0193-15.2015
65. Song, Y. H., Hwang, Y. S., Kim, K., Lee, H. R., Kim, J. H., Maclachlan, C., Dubois, A., Jung, M. W., Petersen, C., Knott, G., Lee, S. H., & Lee, S. H. (2020). Somatostatin enhances visual processing and perception by suppressing excitatory inputs to parvalbumin-positive interneurons in V1. *Science advances*, *6*(17), eaaz0517. https://doi.org/10.1126/sciadv.aaz0517
66. Soumier, A., & Sibille, E. (2014). Opposing effects of acute versus chronic blockade of frontal cortex somatostatin-positive inhibitory neurons on behavioral emotionality in mice. *Neuropsychopharmacology : official publication of the American College of Neuropsychopharmacology*, *39*(9), 2252–2262. https://doi.org/10.1038/npp.2014.76
67. Spalding, K. L., Bergmann, O., Alkass, K., Bernard, S., Salehpour, M., Huttner, H. B., Boström, E., Westerlund, I., Vial, C., Buchholz, B. A., Possnert, G., Mash, D. C., Druid, H., & Frisén, J. (2013). Dynamics of hippocampal neurogenesis in adult humans. *Cell*, *153*(6), 1219–1227. https://doi.org/10.1016/j.cell.2013.05.002
68. Spiegel, A. M., Koh, M. T., Vogt, N. M., Rapp, P. R., & Gallagher, M. (2013). Hilar interneuron vulnerability distinguishes aged rats with memory impairment. *The Journal of comparative neurology*, *521*(15), 3508–3523. https://doi.org/10.1002/cne.23367
69. Stanley, D. P., & Shetty, A. K. (2004). Aging in the rat hippocampus is associated with widespread reductions in the number of glutamate decarboxylase-67 positive interneurons but not interneuron degeneration. *Journal of neurochemistry*, *89*(1), 204–216. https://doi.org/10.1111/j.1471-4159.2004.02318.x
70. Steinmetz, J., Christensen, K. B., Lund, T., Lohse, N., Rasmussen, L. S., & ISPOCD Group (2009). Long-term consequences of postoperative cognitive dysfunction. *Anesthesiology*, *110*(3), 548–555. https://doi.org/10.1097/ALN.0b013e318195b569
71. Steward O. (1976). Topographic organization of the projections from the entorhinal area to the hippocampal formation of the rat. *The Journal of comparative neurology*, *167*(3), 285–314. https://doi.org/10.1002/cne.901670303
72. Tamminga, C. A., Foster, N. L., Fedio, P., Bird, E. D., & Chase, T. N. (1987). Alzheimer's disease: low cerebral somatostatin levels correlate with impaired cognitive function and cortical metabolism. *Neurology*, *37*(1), 161–165. https://doi.org/10.1212/wnl.37.1.161
73. Tay, T. L., Savage, J. C., Hui, C. W., Bisht, K., & Tremblay, M. È. (2017). Microglia across the lifespan: from origin to function in brain development, plasticity and cognition. *The Journal of physiology*, *595*(6), 1929–1945. https://doi.org/10.1113/JP272134
74. Tsien, J. Z., Huerta, P. T., & Tonegawa, S. (1996). The essential role of hippocampal CA1 NMDA receptor-dependent synaptic plasticity in spatial memory. *Cell*, *87*(7), 1327–1338. https://doi.org/10.1016/s0092-8674(00)81827-9

75. Vécsei, L., Bollók, I., & Telegdy, G. (1983). Intracerebroventricular somatostatin attenuates electroconvulsive shock-induced amnesia in rats. *Peptides*, *4*(3), 293–295. https://doi.org/10.1016/0196-9781(83)90135-3
76. Viollet, C., Lepousez, G., Loudes, C., Videau, C., Simon, A., & Epelbaum, J. (2008). Somatostatinergic systems in brain: networks and functions. *Molecular and cellular endocrinology*, *286*(1-2), 75–87. https://doi.org/10.1016/j.mce.2007.09.007
77. von Bohlen und Halbach, O., Zacher, C., Gass, P., & Unsicker, K. (2006). Age-related alterations in hippocampal spines and deficiencies in spatial memory in mice. *Journal of neuroscience research*, *83*(4), 525–531. https://doi.org/10.1002/jnr.20759
78. Yuan, M., Meyer, T., Benkowitz, C., Savanthrapadian, S., Ansel-Bollepalli, L., Foggetti, A., Wulff, P., Alcami, P., Elgueta, C., & Bartos, M. (2017). Somatostatin-positive interneurons in the dentate gyrus of mice provide local- and long-range septal synaptic inhibition. *eLife*, *6*, e21105. https://doi.org/10.7554/eLife.21105

A

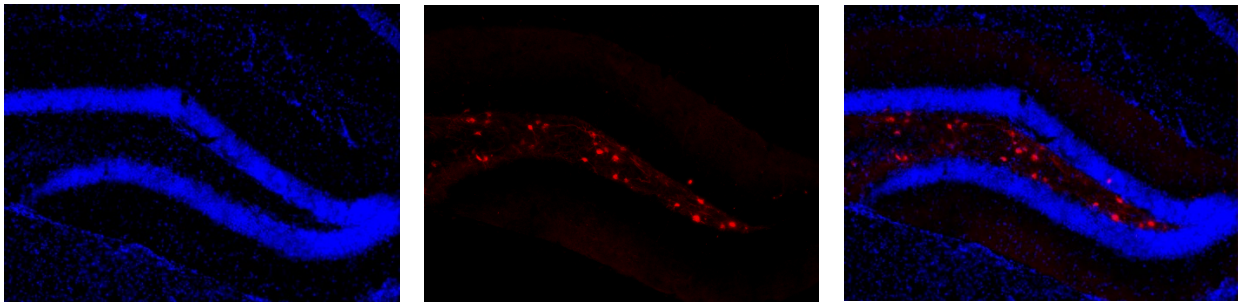

B

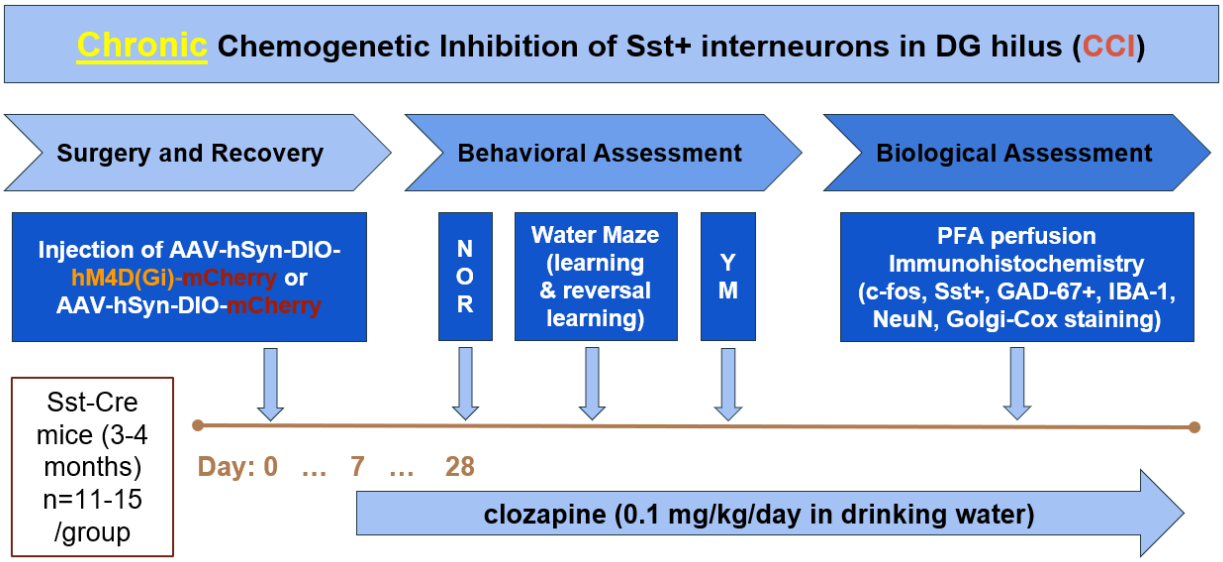
Chronic Chemogenetic Inhibition of Sst+ interneurons in DG hilus (CCI)
Surgery and Recovery
Behavioral Assessment
Biological Assessment
Injection of AAV-hSyn-DIO-hM4D(Gi)-mCherry or AAV-hSyn-DIO-mCherry
N O R
Water Maze (learning & reversal learning)
Y M
PFA perfusion Immunohistochemistry (c-fos, Sst+, GAD-67+, IBA-1, NeuN, Golgi-Cox staining)
Sst-Cre mice (3-4 months) n=11-15 /group
Day: 0 … 7 … 28
clozapine (0.1 mg/kg/day in drinking water)

C

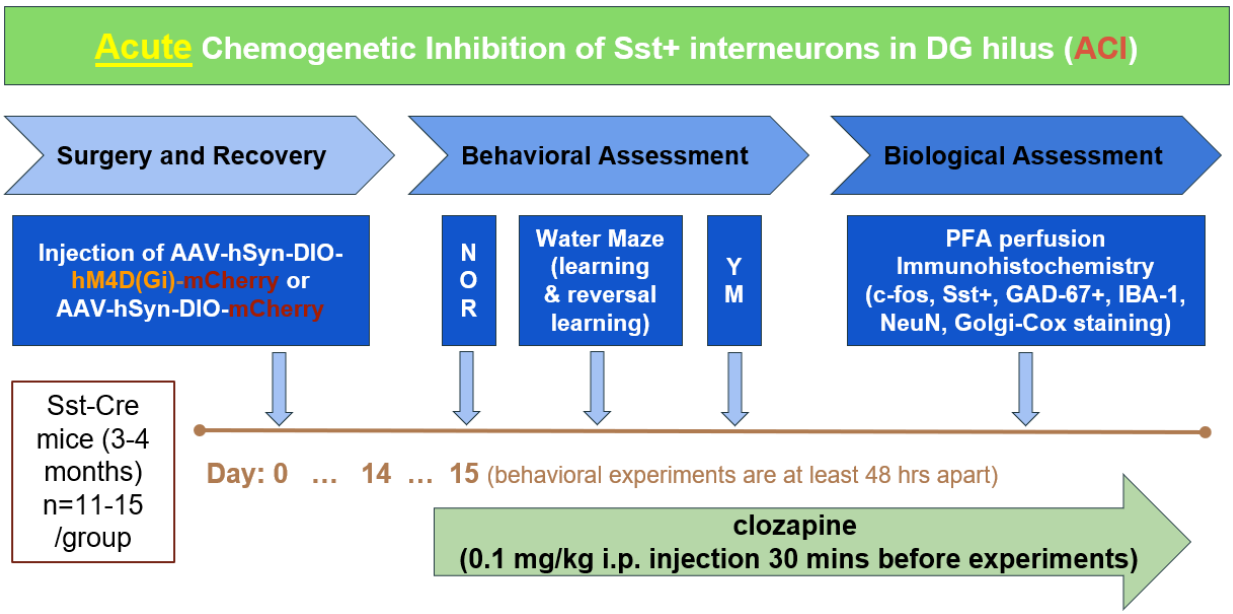
Acute Chemogenetic Inhibition of Sst+ interneurons in DG hilus (ACI)
Surgery and Recovery
Behavioral Assessment
Biological Assessment
Injection of AAV-hSyn-DIO-hM4D(Gi)-mCherry or AAV-hSyn-DIO-mCherry
N O R
Water Maze (learning & reversal learning)
Y M
PFA perfusion Immunohistochemistry (c-fos, Sst+, GAD-67+, IBA-1, NeuN, Golgi-Cox staining)
Sst-Cre mice (3-4 months) n=11-15 /group
Day: 0 … 14 … 15 (behavioral experiments are at least 48 hrs apart)
clozapine (0.1 mg/kg i.p. injection 30 mins before experiments)

Figure 1. Experimental design of DG hilus somatostatin-positive (Sst^+) cell manipulation. ***A,*** Immunofluorescence staining of coronal sections from an AAV-mCherry mouse showing DAPI counterstain (left: DAPI; middle: mCherry expression; right: merged image)." ***B,*** Top, Chronic chemogenetic inhibition of DG hilus SST^+ cells. Bottom, Acute chemogenetic inhibition of DG hilus SST^+ cells.

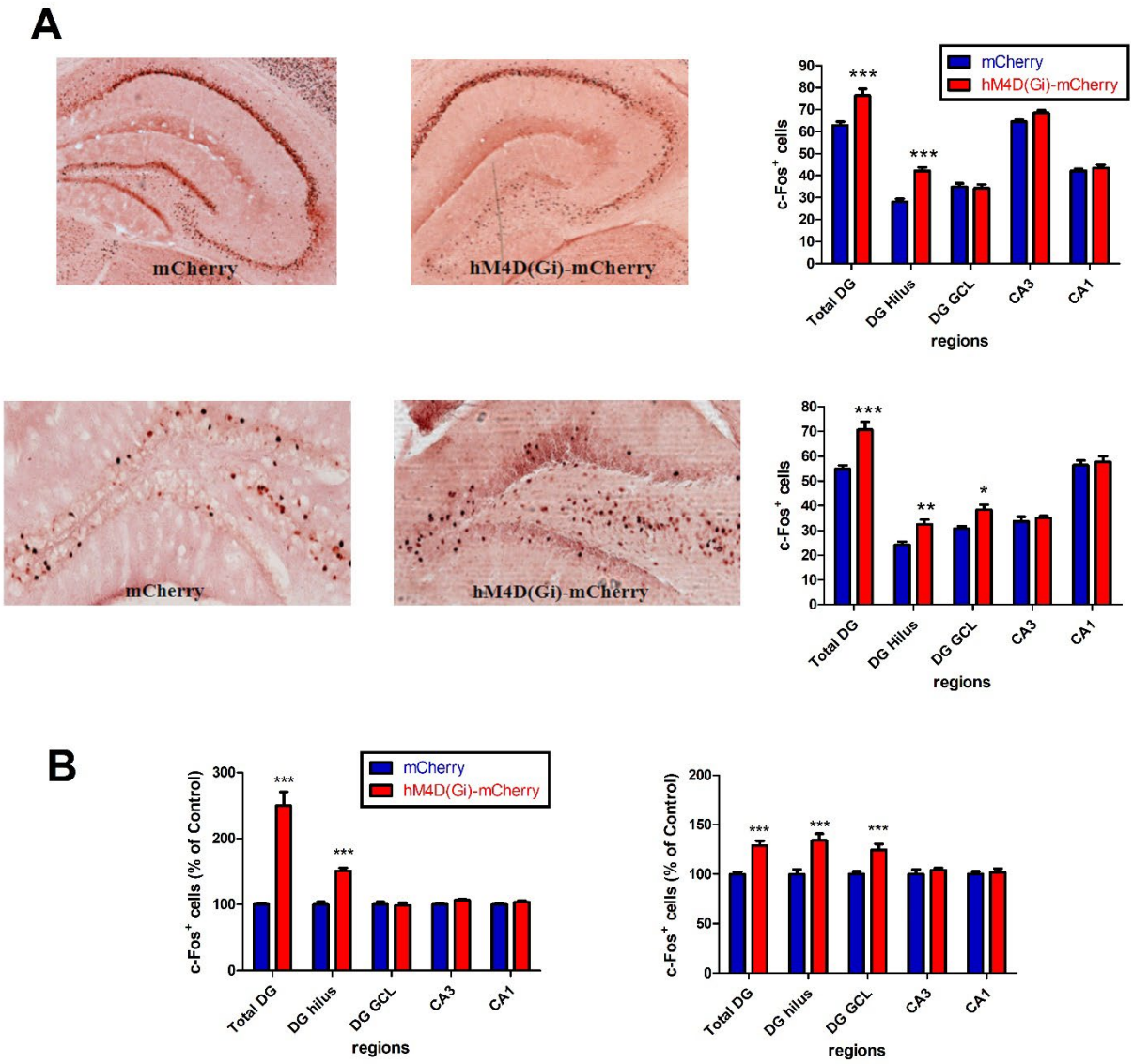

Figure 2. c-Fos$^+$ cell counts in hippocampal subfields (Total DG, DG hilus, DG granule cell layer (DG GCL), CA3, CA1). ***A,*** Top, Representative sections showing c-Fos$^+$ expression in AAV-mCherry mice and AAV-hM4D(Gi)-mCherry mice during chronic chemogenetic inhibition (CCI). Bottom, Representative sections showing c-Fos$^+$ expression in AAV-mCherry and AAV-hM4D(Gi)-mCherry mice during acute chemogenetic inhibition (ACI). ***B,*** Left, Estimated density of c-Fos$^+$ cells in AAV-hM4D(Gi)-mCherry mice expressed as percentage of AAV-mCherry mice during CCI. Right, Estimated density of c-Fos$^+$ cells in AAV-hM4D(Gi)-mCherry mice expressed as percentage of AAV-mCherry mice during ACI. *$p<0.05$, **$p<0.01$, ***$p<0.001$ compared with the corresponding AAV-mCherry group.

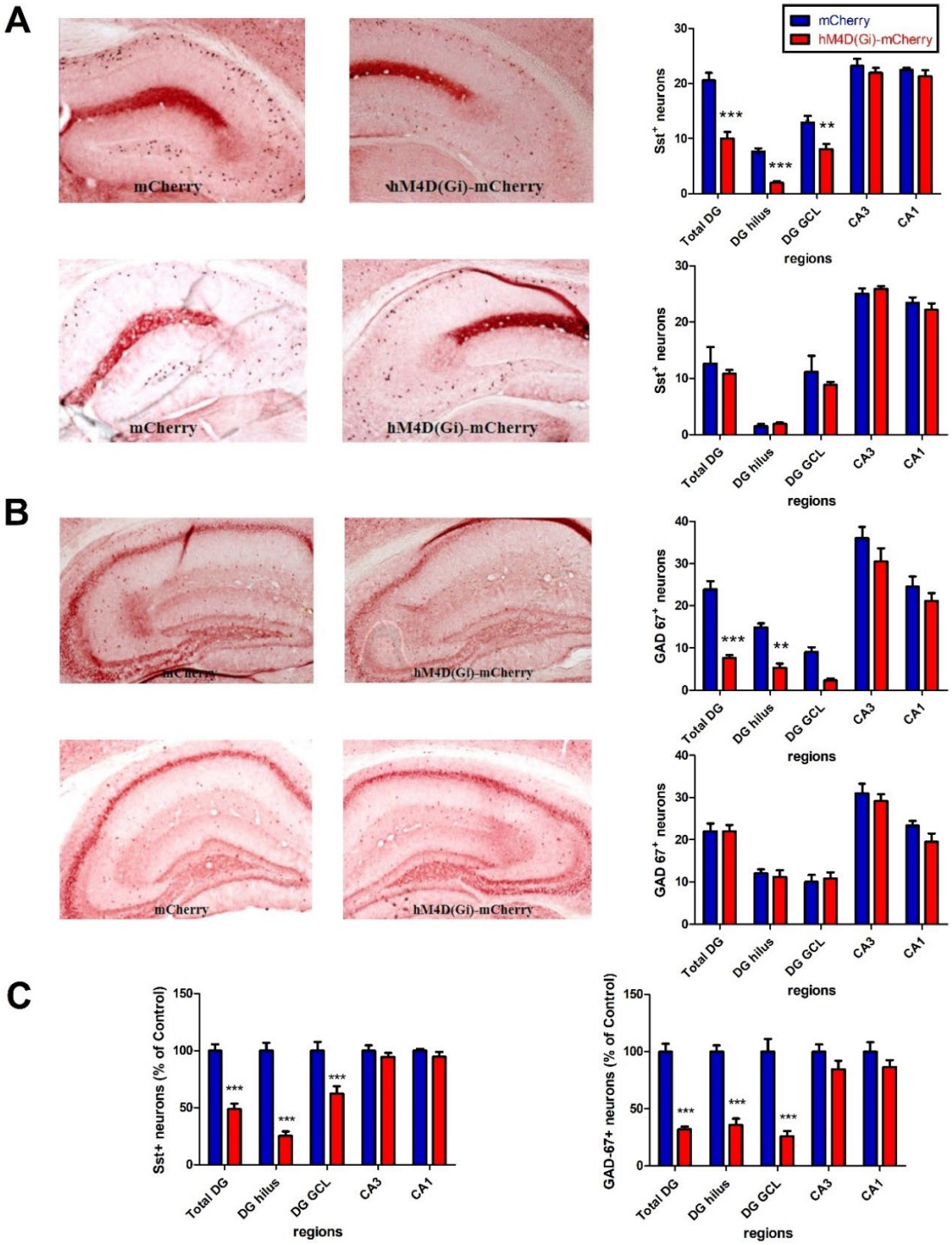

Figure 3. Sst$^+$ neuron and GAD67$^+$ neuron counts in hippocampal subfields. ***A,*** Top, Representative sections showing Sst$^+$ expression in AAV-mCherry and AAV-hM4D(Gi)-mCherry mice during CCI. Bottom, Sst$^+$ expression during ACI. ***B,*** Top, Representative sections showing GAD-67$^+$ expression in AAV-mCherry and AAV-hM4D(Gi)-mCherry mice during CCI. Bottom, GAD-67$^+$ expression during ACI. ***C,*** Left, Estimated density of Sst$^+$ neurons in AAV-hM4D(Gi)-mCherry mice expressed as percentage of AAV-mCherry mice during CCI.

Right, Estimated density of GAD-67^{+} cells in AAV-hM4D(Gi)-mCherry mice expressed as percentage of AAV-mCherry mice during CCI. *$p<0.05$, **$p<0.01$, ***$p<0.001$

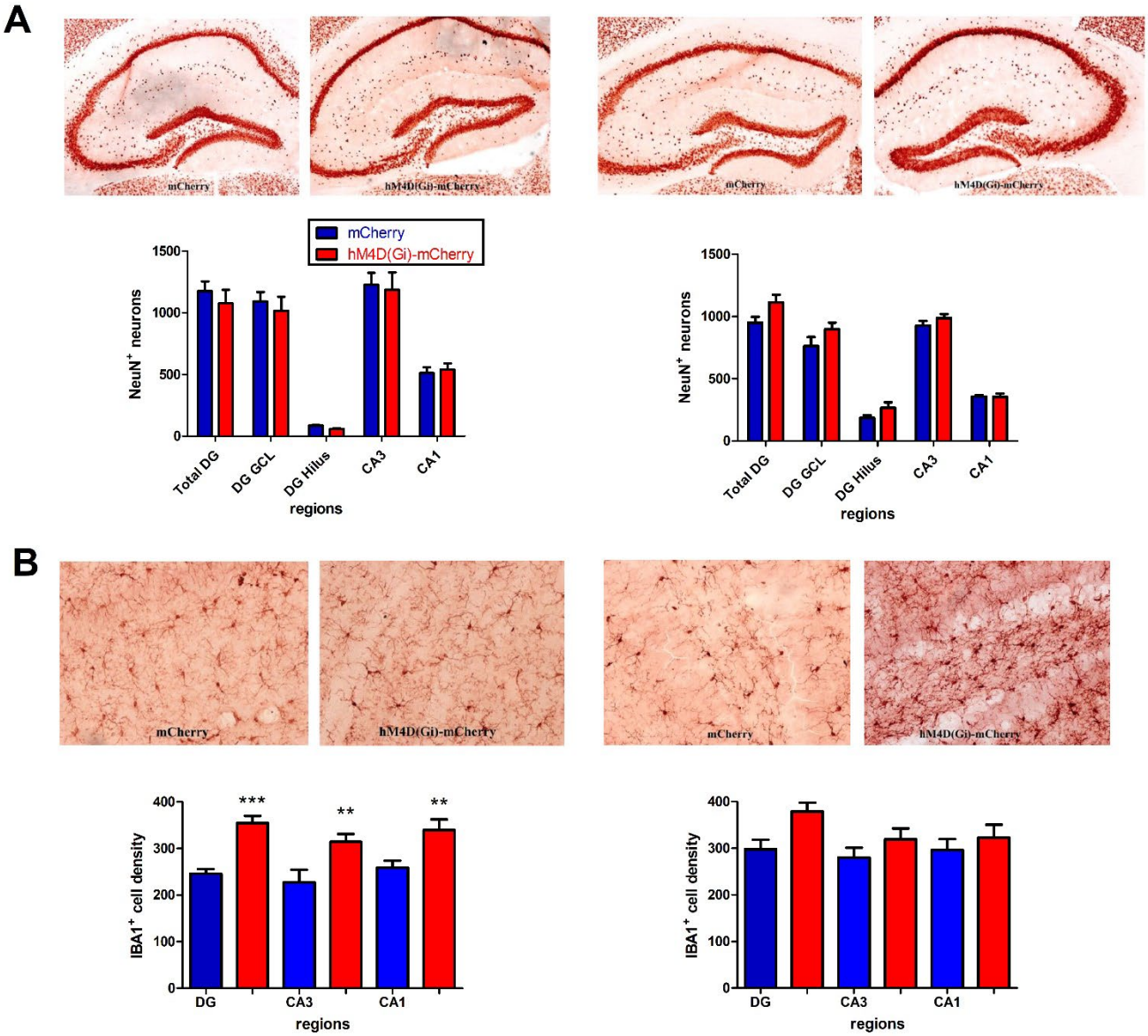

Figure 4. NeuN+ neuron counts and IBA-1+ cell density analysis in hippocampal subfields. ***A,*** Left, Representative sections showing NeuN$^+$ (total neurons) expression in mCherry and hM4D(Gi)-mCherry mice during CCI. Right, NeuN$^+$ neurons expression during ACI. ***B,*** Left, Representative sections showing IBA1$^+$ cell density in mCherry and hM4D(Gi)-mCherry mice during CCI. Right, Representative sections showing IBA1$^+$ cell density in mCherry and hM4D(Gi)-mCherry mice during ACI. *$p<0.05$, **$p<0.01$, ***$p<0.001$

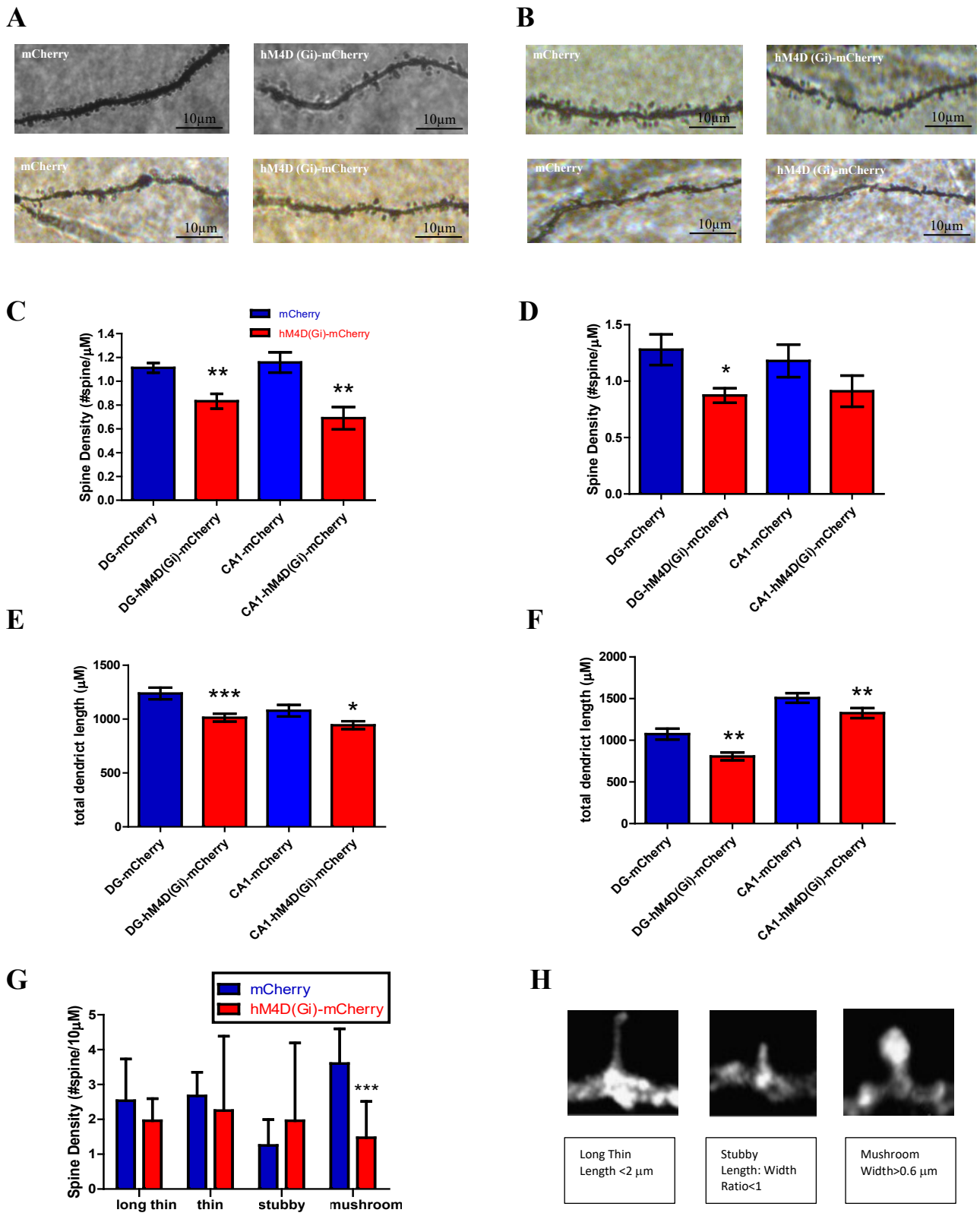
A
mCherry
hM4D (Gi)-mCherry
10μm
B
C
mCherry
hM4D(Gi)-mCherry
Spine Density (#spine/μM)
DG-mCherry
DG-hM4D(Gi)-mCherry
CA1-mCherry
CA1-hM4D(Gi)-mCherry
D
E
total dendrict length (μM)
F
G
Spine Density (#spine/10μM)
long thin
thin
stubby
mushroom
H
Long Thin
Length <2 μm
Stubby
Length: Width
Ratio<1
Mushroom
Width>0.6 μm

Figure 5. Morphological features of DG and CA1 regions in the hippocampus after CCI and ACI. ***A,*** Top, Representative pictures of CCI in DG dendrite and spine morphologies used for quantification with a 100x objective. Bottom, Representative pictures of CCI in CA1 dendrite and spine morphologies used for quantification with a 100x objective. ***B,*** Top, Representative pictures of ACI in DG dendrite and spine morphologies used for quantification with a 100x objective. Bottom, Representative pictures of ACI in CA1 dendrite and spine morphologies used for quantification with a 100x objective. ***C,*** Spine density in DG and CA1 after CCI. ***D,*** Spine density in DG and CA1 after ACI. ***E,*** Total dendritic length in DG and CA1 after CCI. ***F,*** Total dendritic length in DG and CA1 after ACI. ***G,*** Density of different spine types after CCI in DG. ***H,*** Top, Examples of long thin, stubby, and mushroom spines. Bottom, Quantification classification of different morphological spine types. *$p<0.05$, **$p<0.01$, ***$p<0.001$ compared with the corresponding AAV-mCherry group.

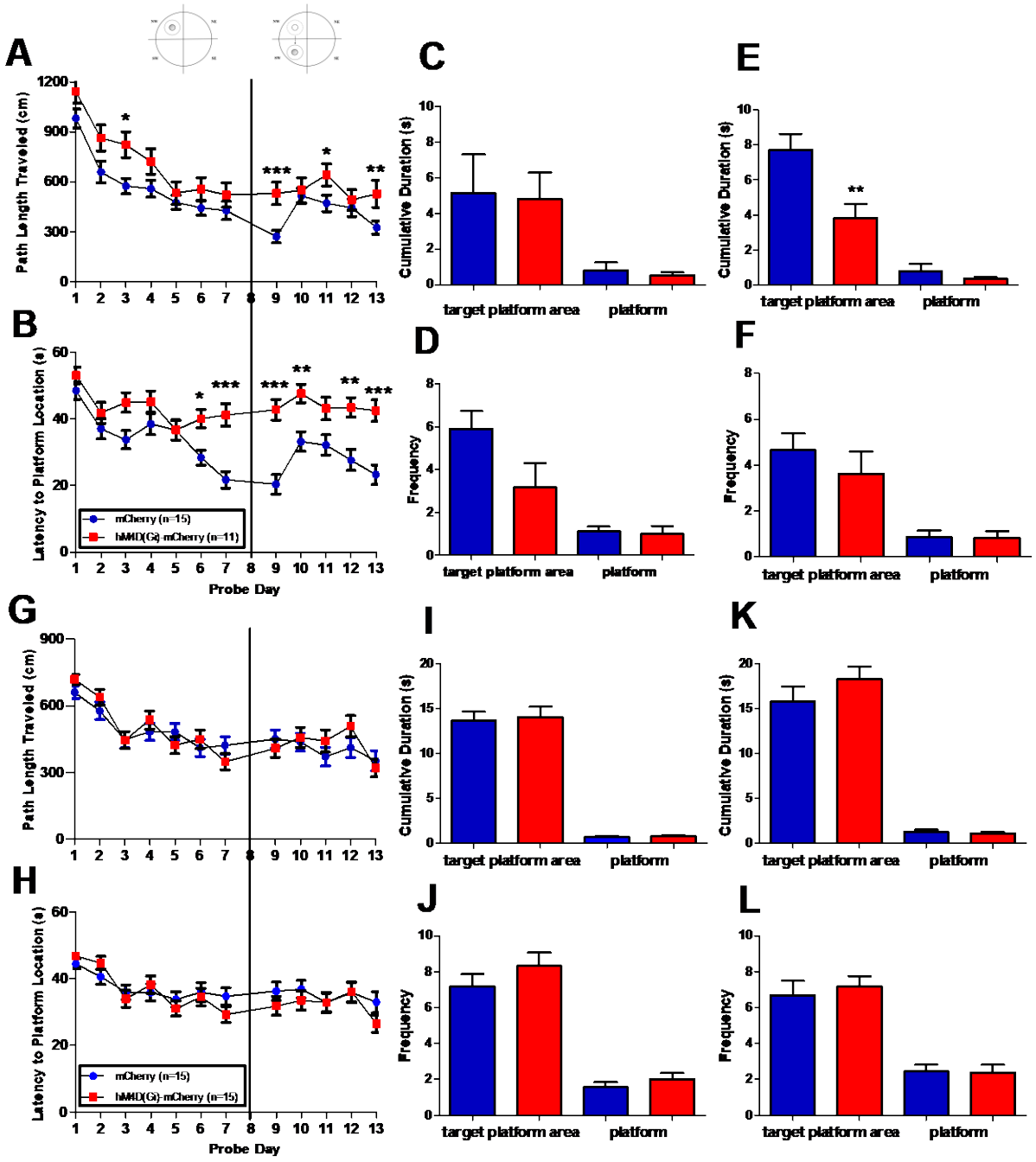

Figure 6. Morris water maze in AAV-mCherry and AAV-hM4D(Gi)-mCherry mice. day1-7, learning phase; day8, learning phase probe trials; day9-13, reversal learning phase; day14, reversal learning probe trials. ***A-F,*** Chronic Chemogenetic Inhibition (CCI). ***A,B,*** Path length and latency to the hidden platform. ***C,D,*** Cumulative duration and frequency to enter target platform area or the platform in learning phase probe trials. ***E,F,*** Cumulative duration and frequency to enter target platform area or the platform in reversal learning phase probe trials. ***G-***

L, Acute Chemogenetic Inhibition (ACI). ***G,H,*** Path length and latency to hidden platform. ***I,J,*** Cumulative duration and frequency to enter target platform area or the platform in learning phase probe trials. ***K,L,*** Cumulative duration and frequency to enter target platform area or the platform in reversal learning phase probe trials. *$p<0.05$, **$p<0.01$, ***$p<0.001$.

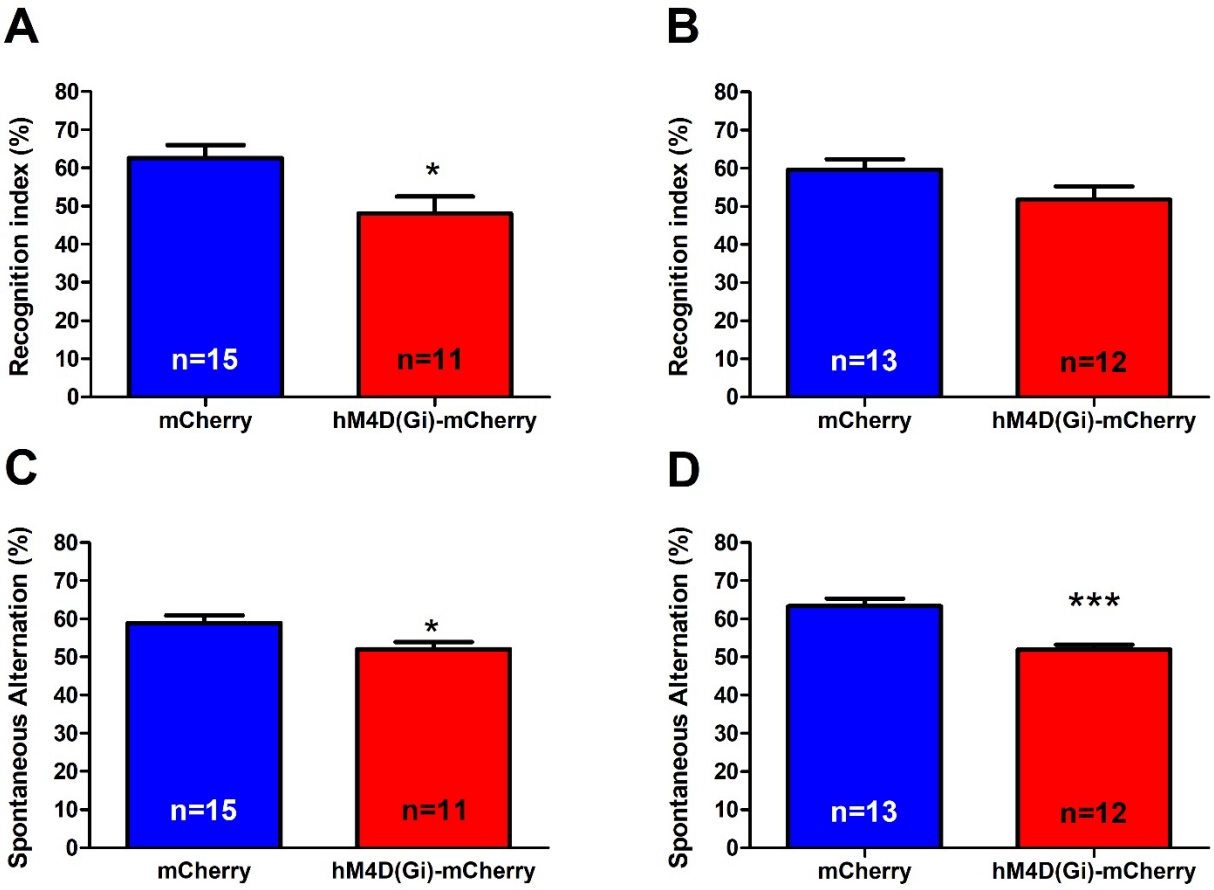

Figure 7. Novel Object Recognition Task (NOR) and Y-maze Task (YM) in AAV-mCherry and AAV-hM4D(Gi)-mCherry mice. ***A,*** Recognition index in NOR in CCI. ***B,*** Recognition index in NOR in ACI. ***C,*** Spontaneous arm alternation percentage in YM in CCI. ***D,*** Spontaneous arm alternation percentage in YM in ACI. *p<0.05, **p<0.01, ***p<0.001.

	c-Fos$^+$	Sst$^+$	GAD-67$^+$	Microglia activation	MWM	NOR	YM
CCI	↑	↓	↓	↑	↓	↓	↓
ACI	↑	–	–	–	–	–	↓

Table 1. Effects of chronic chemogenetic inhibition of DG hilus Sst$^+$ interneurons (CCI) and acute chemogenetic inhibition of DG hilus Sst$^+$ interneurons (ACI). The displayed results are comparing outcomes in AAV-hM4D(Gi)-mCherry mice compared to AAV-mCherry mice.

	CCI spine density	ACI spine density	CCI dendritic length	ACI dendritic length
DG	↓	↓	↓	↓
CA1	↓	–	↓	↓

Table 2. Spine density and dendritic length of DG and CA1 region in the hippocampus after CCI and ACI, except for spine density in CA1 region in ACI. The displayed results are comparing outcomes in AAV-hM4D(Gi)-mCherry mice compared to AAV-mCherry mice.